

# Perovskite Emitters as a Platform Material for Down-Conversion Applications

Hyeokjae Lee, Jinwoo Park, Sungjin Kim, Seung-Chul Lee, Young-Hoon Kim, and Tae-Woo Lee\*

Methods to overcome the instability of perovskites to moisture, light, and heat in down-converted displays (DCDs), in which films of perovskite emitters are placed on top of the backlight unit and convert its light to a desired color, are reviewed here. First, the photophysical properties of perovskite emitters as light converters in DCDs are discussed. Second, five strategies to improve stability of perovskite emitting materials (PeMs) mostly in a form of perovskite nanoparticles (PeNPs) are summarized: i) encapsulation in inorganics, ii) encapsulation in polymer, iii) semiconductor shelling, iv) ligand engineering, and v) defect engineering. Third, examples of DCDs that use perovskite emitters are presented. Finally, future perspectives for the commercialization of perovskite emitters as a next-generation material that can be applied to DCDs are outlined.

## 1. Introduction

Most flat-panel displays other than self-emissive displays such as organic light-emitting diodes contain a light source called a backlight unit (BLU). Conventional BLU especially for liquid crystal displays (LCDs) does not include separate light sources

for the red, green, and blue (RGB) colors but incorporates white light sources, which can be further converted to RGB emission using color filters (CFs). Recent commercialized televisions and computer monitors generally use down-converted displays (DCDs), in which color conversion phosphor films and CFs are laid atop the blue BLU to change its emission to the desired color. Semiconductor nanoparticles (NPs) such as cadmium (Cd) quantum dots (QDs) and indium phosphide (InP) QDs with narrow spectral bandwidth, high luminous efficiency, and easy tunable wavelength have been recently introduced as more suitable materials for display application than the yttrium aluminum

garnet (YAG) phosphors that are widely used at present. QDs have good color purity, but users demand still higher color purity displays that can represent realistic colors.<sup>[1–7]</sup>

Metal-halide perovskites (shortly, perovskite) have simple crystal structures of  $ABX_3$  or  $A_2BX_4$  (where A is an organic ammonium (e.g., methylammonium (MA;  $CH_3NH_3^+$ ) and formamidinium (FA;  $CH(NH_2)_2^+$ ) or an alkali metal cation (e.g.,  $Cs^+$ ), B is a transition metal cation (e.g.,  $Pb^{2+}$ ), and X is a halide anion ( $I^-$ ,  $Br^-$ , and  $Cl^-$ )<sup>[8]</sup> (Figure 1a). Perovskite emitters have higher color purity (color gamut  $\geq 140\%$  in National Television Standards Committee (NTSC) TV color standard and  $\geq 95\%$  in International Telecommunication Union (ITU) Recommendation Rec. 2020 standard) than inorganic QDs emitters (full width at half maximum (FWHM)  $\approx 30$  nm; color gamut  $\approx 110$ – $115\%$  in NTSC standard and  $< 90\%$  in Rec. 2020 standard). However, perovskite have low exciton binding energy ( $\approx 30$ – $50$  meV in  $MAPbI_3$  and  $\approx 76$  meV in  $MAPbBr_3$ ), so most of electron–hole pairs are dissociated into free charge carriers, reducing radiative recombination and photoluminescence quantum yield (PLQY) at room temperature.

Perovskite nanoparticles (PeNPs) are highly bright<sup>[8]</sup> and have unique optical and physical properties such as facile emission wavelength tunability, narrow FWHM, and high PLQY ( $\geq 95\%$ ) compared to inorganic QDs and organic emitters (Figure 1b)<sup>[8]</sup> and high absorption coefficient compared to inorganic QDs. Therefore, many researchers have tried to use them as light emitters. However, perovskite emitters have limitations when applied to DCDs. First, polar organic solvents or water cause structural changes in perovskites and consequent loss of optical properties. Second, environmental factors such as moisture, heat, light, and oxygen degrade perovskite emitters.


Dr. H. Lee, J. Park, S. Kim, Dr. S.-C. Lee, Dr. Y.-H. Kim, Prof. T.-W. Lee  
 Department of Materials Science and Engineering  
 Seoul National University  
 1 Gwanak-ro, Gwanak-gu, Seoul 08826, Republic of Korea  
 E-mail: twlees@snu.ac.kr

Dr. H. Lee  
 Research Institute of Advanced Materials  
 Seoul National University  
 1 Gwanak-ro, Gwanak-gu, Seoul 08826, Republic of Korea

Prof. T.-W. Lee  
 BK21 PLUS SNU Materials Division for Educating Creative Global Leaders  
 Seoul National University  
 1 Gwanak-ro, Gwanak-gu, Seoul 08826, Republic of Korea

Prof. T.-W. Lee  
 Institute of Engineering Research  
 Research Institute of Advanced Materials  
 Nano Systems Institute (NSI)  
 Seoul National University  
 1 Gwanak-ro, Gwanak-gu, Seoul 08826, Republic of Korea

Prof. T.-W. Lee  
 School of Chemical and Biological Engineering  
 Seoul National University (SNU)  
 1 Gwanak-ro, Gwanak-gu, Seoul 08826, Republic of Korea

 The ORCID identification number(s) for the author(s) of this article can be found under <https://doi.org/10.1002/admt.202000091>.

DOI: 10.1002/admt.202000091

Third, due to the fast exchange of the halide ions that are components of perovskite emitters; when two different color-emitting PeNPs with different halide source are mixed, the intermediate wavelength may be intensified.<sup>[9]</sup> For example, when PeNPs that emit red and green light are dispersed together, the intensity of intermediate emission wavelength of yellow tends to be increased and the emission bandwidth is widened. This increased intensity in intermediate wavelength implies that the excellent optical properties of the perovskite emitter are degraded.<sup>[10]</sup>

To maintain the advantages of perovskite emitters, the stability of each PeNP must be assured, while maintaining the intrinsic optical properties. The photoluminescence (PL) is induced by an external light source and is affected by light-induced heat, high light flux, and the chemical environment that the film encounters when it is dispersed in various polymers or directly deposited on the light-emitting diode (LED). Therefore, structural and interfacial stability, and tolerance to heat, light, and environmental conditions (moisture and oxygen) must be achieved in perovskite-based DCDs.

Here we review the development of perovskite emitters (PeNPs and other perovskite emitting materials (PeMs) in a different form) and demonstrate their potential as light emitters in DCDs. In Section 2, we compare characteristics of perovskite emitters with those of conventional QDs and phosphors that have been used in DCDs. In Section 3, we provide various methods to increase the stability of perovskite emitters by using inorganic oxides, polymers, and inorganic semiconductors. In Section 4, we review applications of perovskite emitters on DCDs. In Section 5, we provide insights and suggest future research directions to further improve DCDs that use perovskite emitters including PeNPs and other types of PeMs.<sup>[8]</sup>

## 2. Next Generation Materials Property Comparison

### 2.1. Commercialization Period

In LCD, organic LED (OLED) and QD, commercialization period of display materials have been shortened with material development (Figure 2). This shortening of the timing of commercialization for new type of panel display makes it possible to expect a faster realization of the next-generation display using perovskite emitters. We compared the periods of commercialization of displays with different materials. The liquid crystal was discovered by Friedrich Reinitzer in 1888,<sup>[11]</sup> but thin film transistor LCD TV<sup>[12]</sup> was introduced in 1982, and after 16 years, it entered the mass production mode; it took about 100 years for commercialization since the first discovery of the liquid crystal material. Organic light-emitting materials were known since the 1960s<sup>[13,14]</sup> and required about 55 years to be released on OLED TVs by LG Electronics Inc. in 2014. Comparing the LCD TV and the OLED TV commercialization periods, it can be seen that it was reduced by about 40 years. After discovering quantum confinement effects by Russian physicist Alexey I. Ekimov<sup>[15]</sup> and discovering that the wavelength could be controlled by size, it took only 30 years for the products to be introduced. As perovskite emitters have advantages in luminescence properties and



**Hyeokjae Lee** received his Ph.D. in electronic engineering from Seoul National University, Korea in 2001. He joined Brain Korea professor at Kookmin University and Chartered Semiconductor Manufacturing (currently GlobalFoundries), Singapore as a senior principle engineer from 2001 to 2006. He has

experience in founding and management of a solution process quantum dots' company. His research focuses on the improvement of optical performance and productivity of inorganic and inorganic–organic hybrid quantum dots.



**Jinwoo Park** is studying for his Ph.D. course and received his B.S. degree in the Department of Materials Science and Engineering of Seoul National University. His current research interest includes synthesis of perovskite quantum dots and perovskite LED fabrication for displays.



**Tae-Woo Lee** is a full professor in materials science and engineering at the Seoul National University, Korea. He received his Ph.D. in chemical engineering from the Korea Advanced Institute of Science and Technology, Korea in 2002. He joined Bell Laboratories, USA as a postdoctoral researcher and worked at Samsung Advanced

Institute of Technology as a member of research staff (2003–2008). He was an associate professor in materials science and engineering at the Pohang University of Science and Technology (POSTECH), Korea until August 2016. His research focuses on printed electronics based on organic and organic–inorganic hybrid materials for flexible displays, solid-state lightings, and solar-energy-conversion devices.

economically superior to conventional QDs, products using PeNPs can be expected to come out sooner.

### 2.2. General Property Comparison

Various emitters have been used in DCDs; these emitters have a range of optical and photophysical properties, reliability,

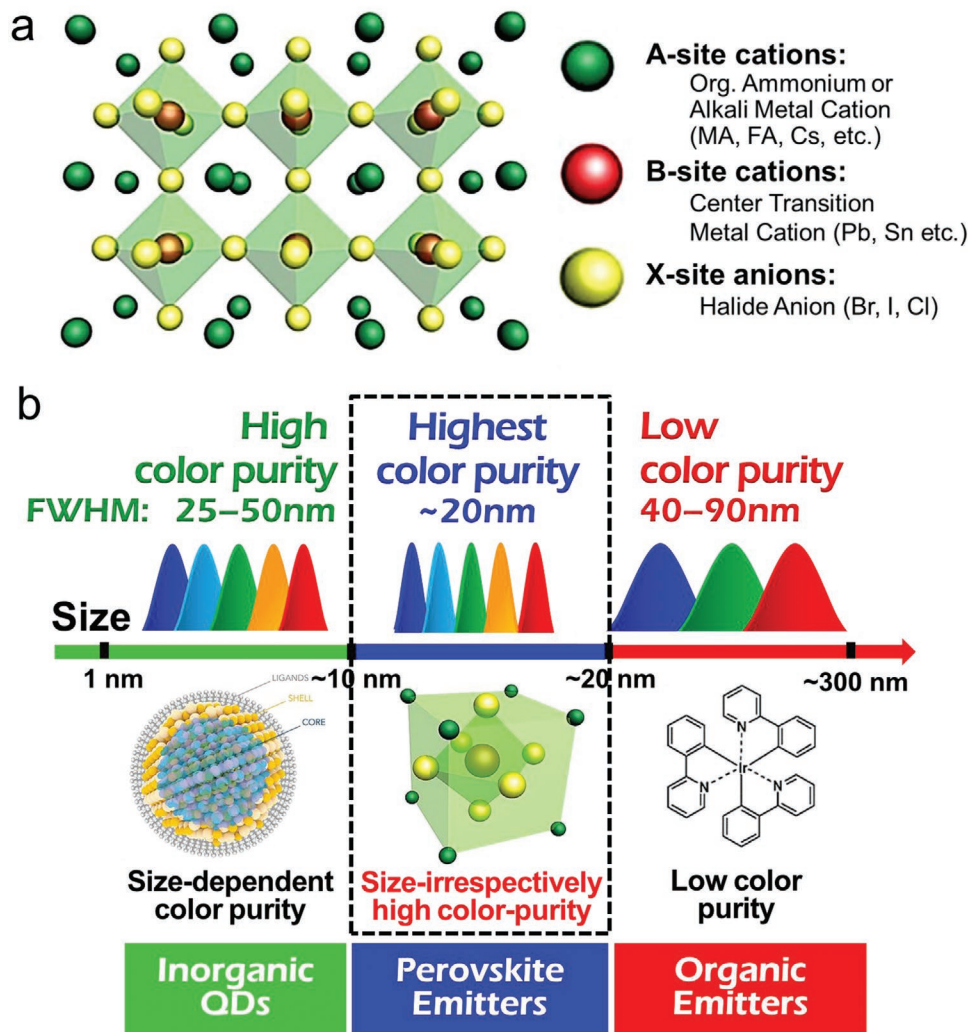


**Figure 1.** a) Schematic of  $ABX_3$  perovskite crystal structure. Reproduced with permission.<sup>[8]</sup> Copyright 2016, National Academy of Sciences and b) schematic representation of emission characteristics, FWHM and size of inorganic QDs, perovskite emitters, and organic emitters.<sup>[8]</sup>

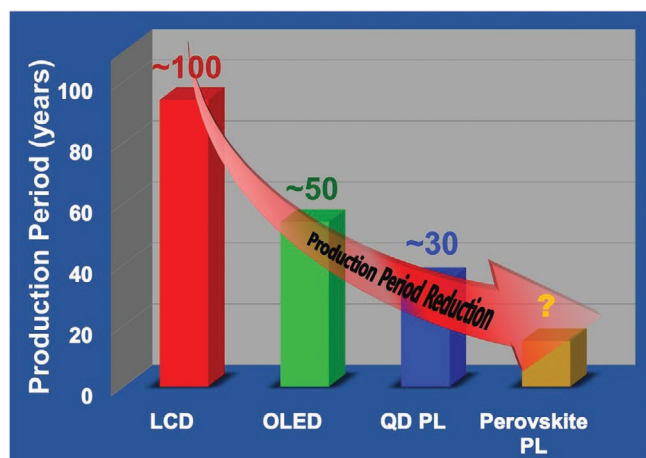


**Figure 2.** Comparison of material discovery for display and release dates of commercial products using found materials. Period of commercialization of liquid crystal, organic materials, and quantum dot, and prediction of perovskite display product period based on them.

and degree of commercialization (Table 1). Most commercialized white LED (WLED) light is obtained by a combination of blue LEDs and YAG:Ce phosphors.<sup>[16–18]</sup> However, the FWHM of WLEDs is  $\approx 70$  nm; this wide band width is the main impediment to its use in display screens that have wide color gamut.<sup>[19,20]</sup>

Material requirements for wide color gamut displays are PLQY > 90%, wide tunable emission wavelength range, and narrow FWHM. InP QDs<sup>[21–26]</sup> have PLQY > 90%, wide tunable emission wavelength range, and FWHM that are generally wider than those of Cd QDs.<sup>[27–31]</sup> PeMs including PeNPs have high absorption coefficients that are 2.5 times higher than that of Cd QDs<sup>[32,33]</sup> and five times higher than that of InP QDs;<sup>[34–40]</sup> these can increase brightness and significantly reduce energy use to maintain the same brightness. Conventional QDs (such as InP QDs, and CdSe QDs) are defect-intolerant structures in which defects exist in localized wide ranges between bandgaps, but perovskite emitters are defect-tolerant structures in which traps exist in the shallow or intra band states of conduction bands. Defects do not act as trap states in perovskite emitters

**Table 1.** Overall characteristics of perovskite, semiconductor nanoparticles, organic phosphors, and conventional inorganic phosphors such as physical properties, optical properties, synthesis method, and long-term stability.

Items	YAG:Ce	White organic	Cd based	InP based	Perovskite
Structure	Micropowder Cerium yttrium aluminum garnet	Micropowder Organic compound	Quantum dot (QD) Core-shell, alloy, gradient	QD Core-shell, gradient	QD, NP, bulk Compound core
	–	–	Covalent bonding	Covalent bonding	Ionic bonding
WL range	550 nm	550 nm	510–630 nm	530–620 nm	450–780 nm
PLQY	≈90%	≈90%	≥90%	≥90%	≥90%
FWHM	70–90 nm	70–90 nm	25–40 nm	35–50 nm	15–25 nm
Absorbance <sup>a)</sup>	– <sup>b)</sup>	– <sup>b)</sup>	0.4	0.2	1
Brightness <sup>a)</sup>	1	0.7	1	≈0.9	1
Fabrication	Ex situ	Ex situ	Ex situ	Ex situ	Ex situ/in situ
Acceleration test <sup>c)</sup>	8585 or 6090	Pass	Pass	Pass	Pass
	8505 or 6005	Pass	Pass	Pass	Pass
	High flux	–	Pass	Pass	On going
Cost <sup>a)</sup>	L	H	M	H	L
Rec.2020	≥60%	≥60%	≈90%	85%	≥95%
RoHS regulation	No issue	No issue	<0.01% (100 ppm)	No issue	<0.1% (1000 ppm)
Production status	Mass	Mass	Mass	Mass	Proto or Lab scale
Synthesis temperature	300–400 °C	100 °C	Hot temp. (HT)	HT	Room temp, HT
Process type	Powder	Deposition	Solution	Solution	Solution/deposition

<sup>a)</sup>Relative comparison; <sup>b)</sup>Specific wavelength absorption; <sup>c)</sup>Industry request condition.

and are therefore benign toward their electronic and optical properties.<sup>[41]</sup>

The consequent reduction in operating cost is a major factor in securing an edge in price competitiveness. PeNPs are easier to be synthesized than inorganic QDs. PeNPs can be synthesized in air at room temperature using methods such as solvent-induced reprecipitation, ligand-assisted reprecipitation, emulsion process, and template assisted synthesis,<sup>[42]</sup> whereas conventional QDs are synthesized at high temperature (200–350 °C) under inert condition in reactors.

Both PeNPs and Cd QDs contain toxic heavy metals. Conventionally developed PeNPs include Pb, which is allowed to constitute ≤1000 ppm of the weight of the display, whereas the Cd in Cd QDs can only constitute ≤100 ppm of the weight of the display by European Union's (EU) Restriction on Hazardous Substances (RoHS) Directive.<sup>[43]</sup> Therefore, PeNPs can be more easily applied than Cd QDs on LEDs. Furthermore, lead-free PeNPs (e.g., (C<sub>4</sub>N<sub>2</sub>H<sub>14</sub>Br)<sub>4</sub>SnBr<sub>6</sub>) have been developed and have achieved PLQY = 95%.<sup>[44,45]</sup>

PeNPs have a higher absorption coefficient than Cd QDs, so the required number of PeNPs is only 1/3 to 1/2 of the number of Cd QDs to achieve the same brightness. PeNPs can reduce the production cost and heavy metal content compared to Cd QDs to meet the RoHS Directive.<sup>[43]</sup>

PeNPs need to meet the basic acceleration-harsh assessment to achieve the reliability that is required by the industry; these assessments include combinations of high temperature and high humidity, high temperature and low humidity<sup>[39]</sup> or high light intensity.<sup>[46,47]</sup> PeNPs fulfill most of the requirements for commercialization. However, perovskites<sup>[48,49]</sup> are

still chemically unstable under some environmental conditions; research is underway to solve this problem.

Nonetheless, the PL properties of PeNPs achieved 135% of the NTSC standard (Figure 3),<sup>[50]</sup> which is superior to commercialized OLEDs and QLEDs. This advantage means that PeNPs have a great potential for use as down-conversion materials in displays.

### 3. Passivation Engineering for PL Applications

Degradation mechanism of PeNPs can vary depending on their composition. Especially A-site cation is a key parameter to control the degradation mechanism; thus engineering of A-site cation is effective to enhance the stability. For example, organic A-site cation, e.g., MA<sup>+</sup> and FA<sup>+</sup>, can be easily decomposed to volatile products such as methylamine, methyl halide, or formamidine.<sup>[51–53]</sup> Therefore, PeNPs with organic A-site cations suffer from instability against thermal stress. It is notable that the degradation of PeNPs can start <100 °C while the decomposition temperature of MA<sup>+</sup> or FA<sup>+</sup> is > 200 °C.<sup>[54,55]</sup>

Another important influence of A-site cation is structural stability. Goldschmidt tolerance factor (*t*) is an important parameter to determine the structural stability, which is expressed by following equation:  $t = \frac{R_A + R_X}{\sqrt{2}(R_B + R_X)}$  (*R<sub>A</sub>* is the radius of A-site cation, *R<sub>B</sub>* is the radius of B-site cation, and *R<sub>X</sub>* is the radius of X-site anion). Radius dependence of Goldschmidt tolerance factor indicates that the appropriate selection of A-site cations for different halides (Cl, Br, I) is important for stability

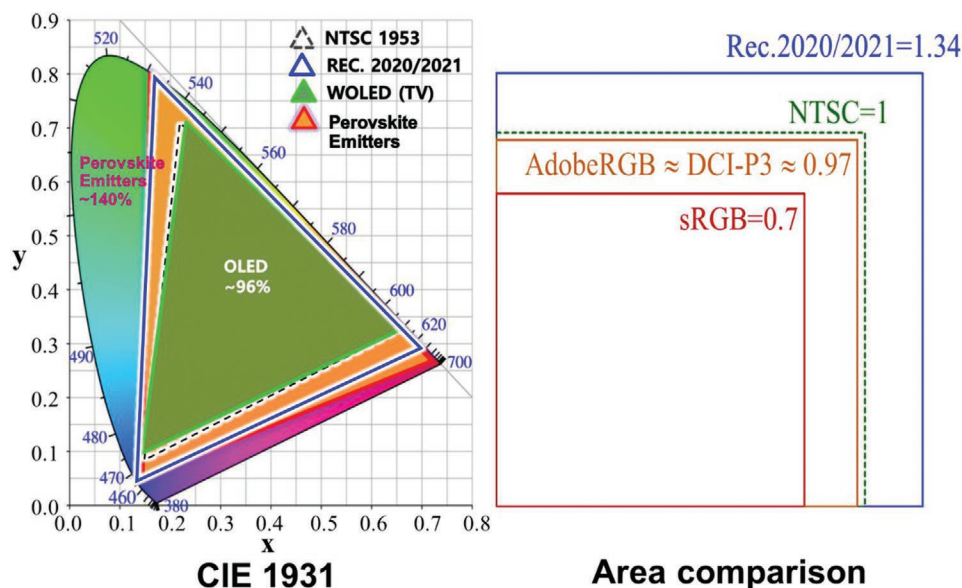


**Figure 3.** White OLED (WOLED) TV<sup>[50]</sup> achieved 96% of NTSC standard, and perovskite emitters achieved 140% wider color reproduction characteristics than the WOLED. Rec.2020/2021 with the widest color space has 34% more space than NTSC 1953. The standard broadcasting signal recommended by ITU to shining a light on a wide color gamut display. To meet this need, display-related companies have been working to develop wide color gamut technologies and seek partnerships with other companies.

enhancement.<sup>[56]</sup> Typically for CsPbI<sub>3</sub> perovskites where Cs cation is too small to stabilize the PbI<sub>6</sub> octahedra, bright black-phase  $\alpha$ -CsPbI<sub>3</sub> can be easily transformed to nonemissive yellow-phase  $\delta$ -CsPbI<sub>3</sub>.<sup>[57]</sup> Mixed A-cation can induce the change of the lattice constant following Vegard's law,<sup>[58,59]</sup> thus stabilize the perovskite crystal and enhance the stability. This stability enhancement was observed in various system including MA/Cs,<sup>[60]</sup> FA/Cs,<sup>[58,61]</sup> and Cs/Rb.<sup>[62,63]</sup>

PeNPs are unstable possibly due to their ionic bond nature; perovskite crystals are easily decomposed under the exposure to light, moisture, oxygen, and heat<sup>[64]</sup> in common regardless of A-site cation. This low stability degrades the reliability of devices and components that use PeNPs. Several approaches have been used to increase the stability of PeNPs. Combined with an understanding of the decomposition mechanism under various conditions, we review recent studies on improving the stability of PeNPs. By principle, these strategies can be classified into four types 1) encapsulation of NPs, 2) perovskite shell engineering, 3) ligand engineering, and 4) defect engineering. The performance in down conversion is also summarized.

Various studies are being performed to develop PeNPs that satisfy all requirements of the display industry (Table 1). We focus on PL applications and describe how inorganic materials or polymer are formed on the PeNPs' surface to improve stability<sup>[52,65,66]</sup> while maintaining superior optical properties (Figure 4).

This section reviews recent attempts to increase the chemical stability of PeNPs with understanding of the decomposition mechanism under various conditions, including effects from light, oxygen and moisture, and the structural instability of the PeNPs.

### 3.1. Inorganic Encapsulation

Silica and alumina have been used to protect PeNPs against external oxygen or moisture. However, ionic bonding of

perovskite easily decomposes during silica coating, so the silica coating source and coating conditions must be selected carefully.

One method is to mix presynthesized CsPbBr<sub>3</sub> PeNP with mesoporous silica spheres that have a pore size of 12–15 nm. The resulting composite significantly increased the thermal stability and photostability (Figure 5a).<sup>[67]</sup> The solution of CsPbBr<sub>3</sub> PeNPs is penetrated into the mesoporous silica and heated to remove the solvent and obtain a stable perovskite composite.<sup>[68]</sup> When perovskite precursors directly fill the pores of mesoporous silica and grow inside mesoporous silica templates, the size of the NPs conforms to the size of the pores; the quantum confinement effect occurs and photostability is improved.<sup>[69]</sup> Similar processes that use mesoporous silica film are being tested.<sup>[70]</sup>

Organosilica complexes such as (3-aminopropyl) triethoxysilane (APTES) have been used as both the capping agent for inorganic PeNPs and the precursor for a silica matrix. All chemicals were mixed in a water-free synthesis system to form PeNPs, then the system was opened to the air, APTES captured the trace water vapor and reacted with it before it contacted the NP surface. In this way, a silica matrix was slowly formed and the delicate PeNPs were protected (Figure 5b).<sup>[71]</sup> After the solution was centrifuged, the supernatant was colorless; this state indicated that all the PeNPs had been collected. The precipitate was dried and PeNP/silica composite powder was obtained. The formation of a crosslinked organic silica network in the PeNPs/silica composites was verified<sup>[72]</sup> by examination of a Fourier-transform infrared spectroscopy spectrum. The PLQY of both red-emitting and green-emitting PeNP/silica powder was remarkably stable over time. Over three months, the PLQY of red-emitting PeNPs/silica powder declined by only 5% and the PLQY of the green-emitting PeNPs/silica powder was nearly unchanged for >80 days (Figure 5b). Therefore, one-pot encapsulation of the PeNPs with silica matrix greatly enhanced their air stability.

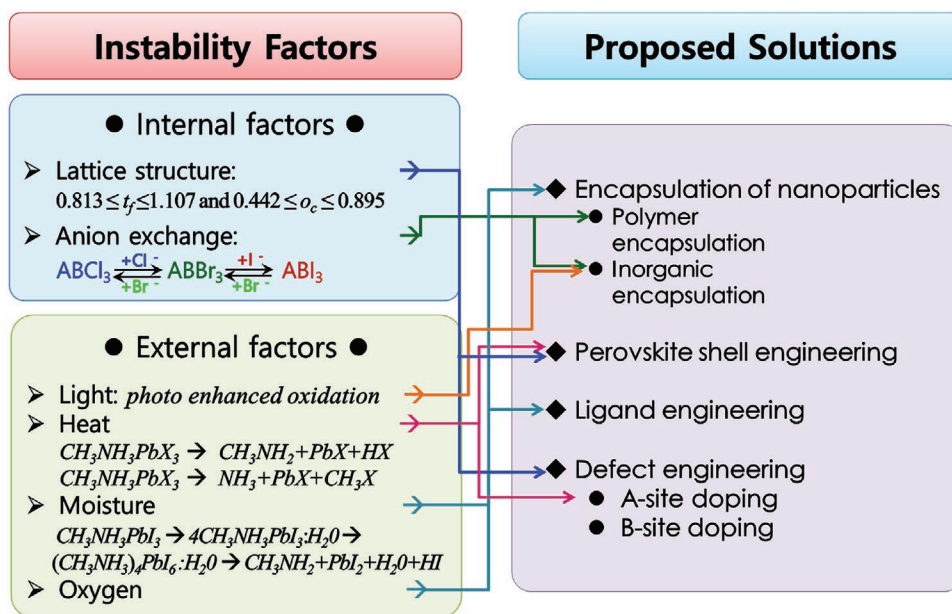


Figure 4. Schematic summary of representative instability of perovskite emitters with chemical reactions<sup>[52,65,66]</sup> and corresponding solutions.

Perhydropolysilazane (PHPS) has been used as a silica precursor to encapsulate inorganic silica rather than organic silica.<sup>[73]</sup> SiO<sub>2</sub> obtained using PHPS exhibited higher chemical stability, hardness, and dense inorganic material than did SiO<sub>2</sub> obtained using tetramethyl orthosilicate and silica obtained using APTES; therefore, the formation of silica barriers by using PHPS provides good resistance to water, heat, and chemicals for PeNPs (Figure 5c). When the temperature is returned from

>100 °C to room temperature, the silica composite recovers its initial PL, whereas the uncoated particles does not recover emitting characteristics. This phenomenon suggests that SiO<sub>2</sub> prevents sintering of CsPbBr<sub>3</sub>-PeNPs and phase transformation of CsPbBr<sub>3</sub> from cubic to orthorhombic, and thereby increases the thermal stability of the CsPbBr<sub>3</sub>-PeNPs.

Other methods include forming CsPbX<sub>3</sub>/SiO<sub>2</sub> compositions by using a water-inducing conversion process combined with

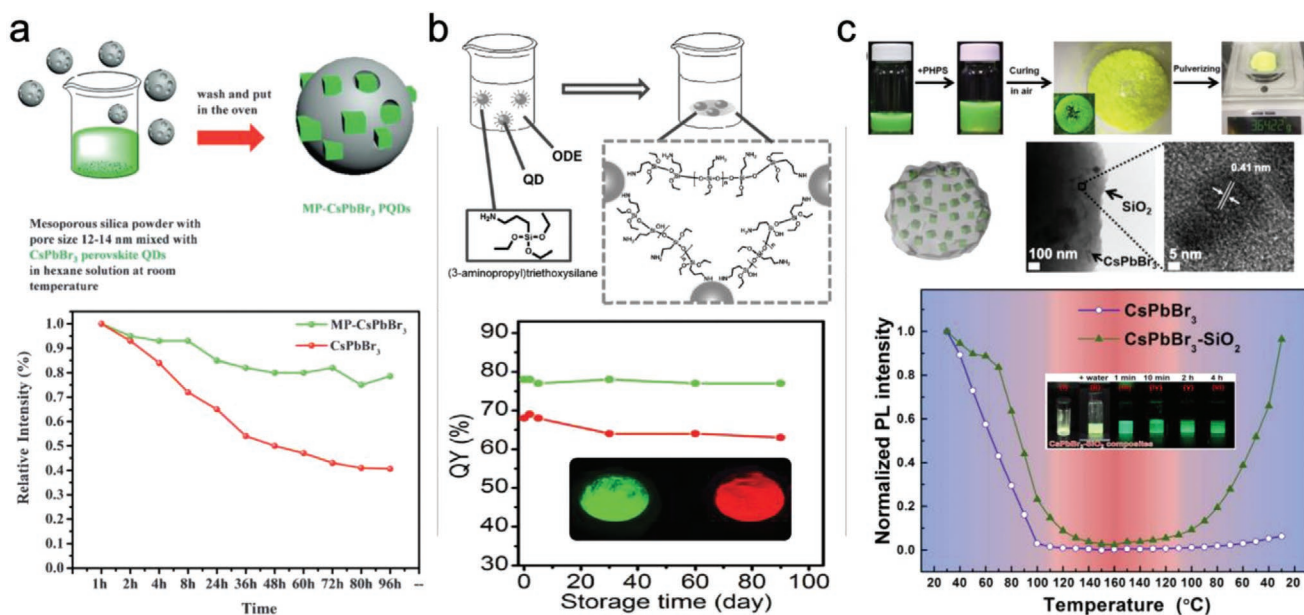


Figure 5. a) Synthesis of mesoporous silica green-emitting PeNPs nanocomposite (MP-PeNPs) and photostability test of MP-CsPbBr<sub>3</sub> and CsPbBr<sub>3</sub>. Reproduced with permission.<sup>[67]</sup> Copyright 2016, Wiley. b) Schematic illustration of formation of PeNPs/silica composites and the PLQY stability of the green-emitting and red-emitting PeNPs/silica composites (inset: photographs of green-emitting and red-emitting PeNPs/silica powders under UV light). Reproduced with permission.<sup>[71]</sup> Copyright 2016, Wiley. c) Procedure to synthesize CsPbBr<sub>3</sub> NP-incorporated PHPS-derived SiO<sub>2</sub> composites, schematic illustration of CsPbBr<sub>3</sub>-SiO<sub>2</sub> composite, temperature-dependent normalized PL intensities of CsPbBr<sub>3</sub> (blue open circle) and CsPbBr<sub>3</sub>-SiO<sub>2</sub> composite (green solid triangle) (inset: photographs of CsPbBr<sub>3</sub>-SiO<sub>2</sub> under UV light). Reproduced with permission.<sup>[73]</sup> Copyright 2016, Elsevier.

a sol–gel protocol,<sup>[74]</sup> and by inserting tetraethyl orthosilicate into the synthesized CsPbBr<sub>3</sub>-PeNPs to create a layer of amorphous silica.<sup>[75]</sup> Other methods of improving the stability use Al<sub>2</sub>O<sub>3</sub><sup>[76,77]</sup> and TiO<sub>2</sub><sup>[78]</sup> as inorganic materials instead of SiO<sub>2</sub>.

### 3.2. Polymer Encapsulation

Polymers can also be used to encapsulate PeMs. Effective encapsulation of PeNPs has improved air stability and water resistance. Moreover, some polymers passivated the surfaces of the NPs and thereby increased their PLQY. Efforts to use polymer materials to improve PeNPs' resistance to moisture and oxygen are continuing.

The polymer matrix that is used for encapsulation must also allow each NP to have a stable emission spectrum from a individual nanocrystal (NC) and must suppress dynamic PL blueshift caused by embedding single NC in a polymeric matrix.<sup>[79]</sup> In particular, polystyrene (PS) provides the best photostability one to two times higher than that obtained by poly(methyl methacrylate) (PMMA), which is a common polymer sealant. Molecular dynamics simulations that use the force-field approximation support the hypothesis that PS provides dense molecular packing on NP surfaces. These findings emphasize that sample fabrication methods can influence the optical properties of PeNPs at the single-particle level and may guide the further design of powerful single-photon sources.

The use of polymer matrices with tailored hydrophobicity, for instance, the use of fluorinated groups, and with improved ligand–polymer interactions with polymers grafted with long alkyl chains can provide high optical characteristics and photostability.<sup>[79]</sup> Perovskite emitters can be coated with a matrix solution. Perovskite emitter precursors are dissolved in dimethylformamide (DMF) solution and then mixed with PS, PMMA, polycarbonate (PC) or acrylonitrile butadiene styrene acetate (ABS), polyvinyl chloride (PVC), and cellulose acetate (CA) in order to form a polymer film. The polymer chains swelled when in contact with a good solvent and finely incorporate precursor solution. During a baking process to remove the solvent, MAPbBr<sub>3</sub> PeNPs formed in the polymer matrix.<sup>[80]</sup> The resulting MAPbBr<sub>3</sub>-PS, MAPbBr<sub>3</sub>-PC, MAPbBr<sub>3</sub>-ABS, MAPbBr<sub>3</sub>-PVC, and MAPbBr<sub>3</sub>-CA films retain high luminescence even when soaked in water for 60 d, but the PL intensity of MAPbBr<sub>3</sub>-PMMA was quenched rapidly possibly due to low swelling ratio of PMMA in DMF solvent (Figure 6a–e).<sup>[80]</sup>

A new approach interfaces CsPbX<sub>3</sub> NPs (X ∈ {Cl, Br, I}) with polymers by copolymerizing methacrylic acid-capped NC (MA-NC) with polyhedral oligomeric silsesquioxane (POSS)-appended methacrylate monomer (MA-POSS) or methyl methacrylate or both (Figure 6f–m).<sup>[81]</sup> The synthesis method for CsPbX<sub>3</sub> NPs uses halide-rich reaction media to enable photopolymerization of comonomers and MA-NC without degrading the NPs. The resulting composite PMMA-co-P(MA-POSS)-co-P(MA-NC) (PMPOPNC) consists of monodispersed NPs

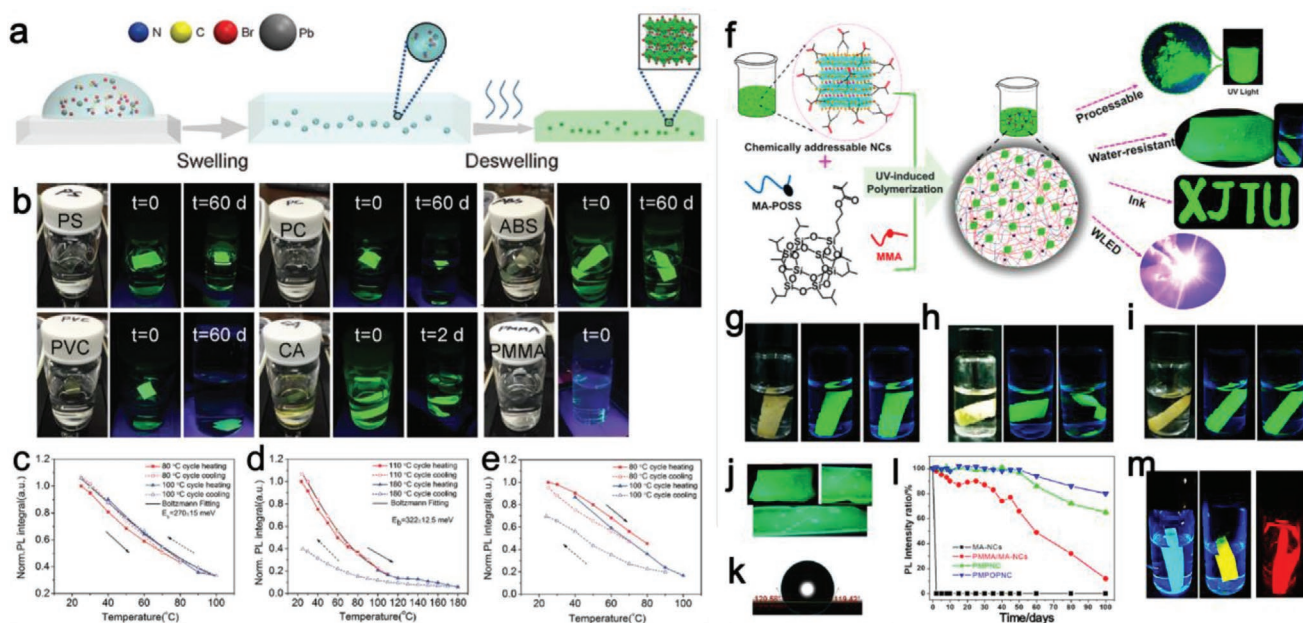


**Figure 6.** a) Scheme of MAPbBr<sub>3</sub>-polymer composite film formation process by swelling–deswelling. Water and thermal stability characterizations. b) Photographs taken under white light or UV irradiation at indicated times. Composite film samples immersed in water are MAPbBr<sub>3</sub>-PS, MAPbBr<sub>3</sub>-PC, MAPbBr<sub>3</sub>-ABS, MAPbBr<sub>3</sub>-PVC, MAPbBr<sub>3</sub>-CA, and MAPbBr<sub>3</sub>-PMMA. Temperature-dependent PL intensity of c) MAPbBr<sub>3</sub>-PS, d) MAPbBr<sub>3</sub>-PC, and e) MAPbBr<sub>3</sub>-ABS. Squares: first thermal cycle; triangles: second thermal cycle. Solid symbols: heating stages; open symbols: cooling stages. Black lines in (c) and (d) indicate Boltzmann fittings for the reversible heating, cooling processes. Reproduced with permission.<sup>[80]</sup> Copyright 2016, Wiley. f) Design of PMPOPNC by copolymerization with chemically addressable NCs. g–i) Photographs taken under ambient light or UV irradiation at indicated times after immersion in water of thin films of g) MA-NC/PMMA blend, h) PMPNC, and i) PMPOPNC films. j,k) Photographs showing the hydrophobicity of PMPOPNC film. l) Relative PLQY plots of MA-NCs, MA-NC/PMMA blend, PMPNC, and PMPOPNC films upon immersion in water over time. m) Photographs of films of PMPOPNC-CspB(Br/Cl)<sub>3</sub>, PMPOPNC-CspB(Br/I)<sub>3</sub>, and PMPOPNC-CspBI<sub>3</sub> taken under UV irradiation after immersion in water for 60 d. Reproduced with permission.<sup>[81]</sup> Copyright 2018, American Chemical Society.

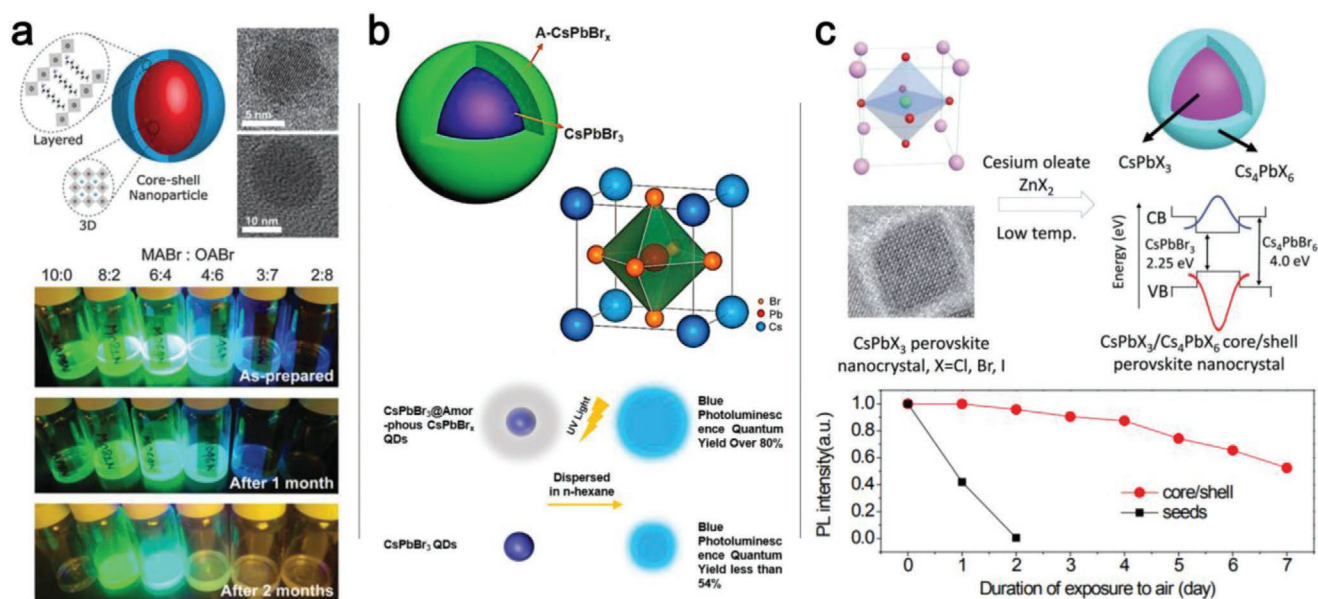


**Figure 7.** a) Schematics showing the core–shell type layer growth of octylammonium lead bromide nanomaterials over MAPbBr<sub>3</sub> NPs. Transmission electron microscope images of core–shell NPs with MABr and OABr molar ratios 8:2 and 3:7. Photographs of mixed organolead bromide perovskite NPs with different MABr–OABr ratios in toluene solution under UV exposure over different time intervals. Reproduced with permission.<sup>[97]</sup> Copyright 2016, Royal Society of Chemistry. b) Diagrams of all-inorganic perovskite CsPbBr<sub>3</sub>@A-CsPbBr<sub>x</sub> composite and structural characterization of perovskite CsPbBr<sub>3</sub>. Reproduced with permission.<sup>[98]</sup> Copyright 2018, American Chemical Society. c) Formation CsPbBr<sub>3</sub>/Cs<sub>4</sub>PbBr<sub>6</sub> core/shell NCs was realized using a seeded growth approach. ZnX<sub>2</sub> (X = Cl, Br, I) was used as a halide source. C<sub>g</sub>: conduction band; V<sub>g</sub>: valence bands; bandgaps were E<sub>g</sub> = 2.25 eV for bulk CsPbBr<sub>3</sub> and E<sub>g</sub> = 4.0 eV for bulk Cs<sub>4</sub>PbBr<sub>6</sub>. Reproduced with permission.<sup>[99]</sup> Copyright 2018, Royal Society of Chemistry.

uniformly distributed within the polymer matrix. The composite shows high PLQY and excellent resistance to water and other protic solvents. The normalized PL of the MA-NCs/PMMA blend thin films decreased to 87% of their initial values after 30 d and to 49%, whereas PMMA-co-P(MA-NC) (PMPNC) and PMPOPNC composite lost less than 5% of PLQY after soaking in water for 60 d (Figure 6f–m).

Other methods synthesized PeNP blends variously in PS or PMMA concentrations to secure absorbance and PLQY characteristics over a certain level.<sup>[72]</sup> PeNP can be encapsulated in macroscale polymers, either PS, poly(laurylmethacrylate) (PLMA), or poly(styrene-ethylene-butylene) (SEBS). PeNP-PS had the best resistance to water and PeNP-PLMA had the best resistance to light; PeNP-SEBS had excellent resistance to both moisture and light.<sup>[82]</sup>

Various other methods have been used to encapsulate perovskite emitters in polymer. Encapsulation method allows individual particle enclosed in polymer, or formation of polymer-perovskite composite film. Many other ways had led to research to increase the chemical stability of PeNPs by using various polymers such as PS,<sup>[83]</sup> PMMA,<sup>[84]</sup> polydimethylsiloxane,<sup>[85]</sup> polyacrylonitrile,<sup>[86]</sup> poly(3,4-ethylenedioxythiophene),<sup>[87]</sup> polyvinylpyrrolidone,<sup>[88]</sup> ethylene vinyl acetate,<sup>[89]</sup> poly(maleic anhydride-alt-1-octadecene),<sup>[90]</sup> poly-2-vinylpyridine (P2VP),<sup>[91]</sup> polystyrene-*b*-poly(ethyl oxide),<sup>[92]</sup> ethyl cellulose,<sup>[93]</sup> carboxybenzene,<sup>[94]</sup> PLMA,<sup>[82]</sup> SEBS,<sup>[82,95]</sup> etc.

### 3.3. Perovskite Shell Engineering

Many researchers have tried to develop PeNPs with ideal core–shell structure similar to CdSe/ZnS or InP/ZnS by

forming a monodispersed crystalline shell on the surface of individual particles. The core/shell particles' size can be smaller than that of NPs coated with polymer or inorganic. The shell can improve the chemical stability of perovskites by preventing oxygen and water from penetrating into the core. A thin shell can improve the luminescence characteristics by passivating the surfaces defects on the core<sup>[4,96]</sup> and reduce the number of nonradiative recombination site.

A solution method can produce highly stable and color-adjustable core–shell type mixed MA–octylammonium (OA) lead bromide PeNPs with spherical shape and high PLQY<sup>[97]</sup> (Figure 7a). The cation ratio in the precursor solution has a major effect on the layered shell growth on PeNP surface, PLQY, and stability of these core-shell PeNPs (stored under ambient conditions at 60% relative humidity (RH)). This structure is a successful development of perovskite/perovskite core/shell NPs; new opportunities to develop inexpensive air-stable and color-tunable perovskite LEDs.

Core/shell structure cubic CsPbBr<sub>3</sub>@amorphous CsPbBr<sub>x</sub> shell perovskite QDs have been obtained using an easy hot injection method and centrifugation process (Figure 7b).<sup>[98]</sup> The core/shell structure QDs showed a highest blue-emission PLQY of 84%, which is much higher than the PLQY of blue-emitting cubic CsPbBr<sub>3</sub> QDs and CsPbBr<sub>x</sub>Cl<sub>3-x</sub> QDs. The amorphous shell protects the perovskite CsPbBr<sub>3</sub> core by enclosing its surface and protecting it against luminescence degradation and also contributes to the formation of excitons; as a result, PLQY increases. These QDs with amorphous shell are free from the defect generated due to lattice mismatch between the core and shell. Therefore, PL efficiency of the original core/shell structure is increased. The amorphous CsPbBr<sub>x</sub> shell can also provide additional protection to prevent oxygen and water from diffusing into the perovskite CsPbBr<sub>3</sub> core.

CsPbX<sub>3</sub>/Cs<sub>4</sub>PbX<sub>6</sub> (X ∈ {Cl, Br, I}) core/shell PeNPs were synthesized by seed growth using an exchange method between CsPbX<sub>3</sub> and Cs<sub>4</sub>PbX<sub>6</sub> (Figure 7c).<sup>[99]</sup> Absorption and X-ray diffraction spectra confirmed that the core/shell structure was formed with a high-energy bandgap shell. The shell's thickness increased smoothly without any evident steps. The initial CsPbBr<sub>3</sub> seeds had PLQY = 84.4%, which is consistent with previously reported values. Core/shell PeNPs that had a thin shell had PLQY = 85% and core-shell PeNPs that had thick shells had PLQY = 96.2%.

The shell increased the chemical stability of the perovskite in air. The PL of the CsPbI<sub>3</sub> PeNPs without the shell was almost quenched within 2 d. The core/shell sample showed only a 47.5% loss of the original value after 7 d. The semiconductor shell is formed on the surface of a core; this method can inspire development of other methods to form core/shell PeNPs to further increase their stability and improve their PL characteristics.

### 3.4. Ligand Engineering

The chemical stability of perovskite emitters can also be increased by ligand engineering. Usually, PeNPs are composed

of a nanometer-scale perovskite crystal surrounded by organic ligands.<sup>[100–104]</sup> Organic ligands can effectively passivate the surface of the perovskite emitters and reduce the nonradiative recombination of spatially confined electron-hole pairs in perovskite crystal.<sup>[70,103,105–109]</sup> Thus the efficiency of PeNPs can be significantly affected by the bonding between perovskite crystal and ligands and strengthening of the bond can increase the chemical stability of PeNPs. Conventional synthesis usually uses a combination of alkyl acid and amine as ligands for PeNPs.<sup>[101–104]</sup> However, protons transfer between carboxylate and ammonium ligands can cause neutralization by Brønsted acid-base equilibria, so ligands can be easily detached from the surface of the perovskite crystal; this process can degrade the PLQY of PeNPs and cause a spectral shift (Figure 8a).<sup>[110–113]</sup>

A new amine-free method (Figure 8b) to synthesize PeNPs with RGB emission (Figure 8c) can increase the oleic acid capped PeNPs' colloidal stability.<sup>[113]</sup> Amine-free synthesis using octyl phosphonic acid (OPA) can actively interact with lead atoms in perovskite crystals, so OPA capped PeNP can maintain PLQY > 90%.<sup>[114]</sup> In particular, OPA-capped PeNP maintained high PLQY even after multiple purification processes; this result indicates that the binding between the perovskite crystal and the ligand was strengthened. Correspondingly,

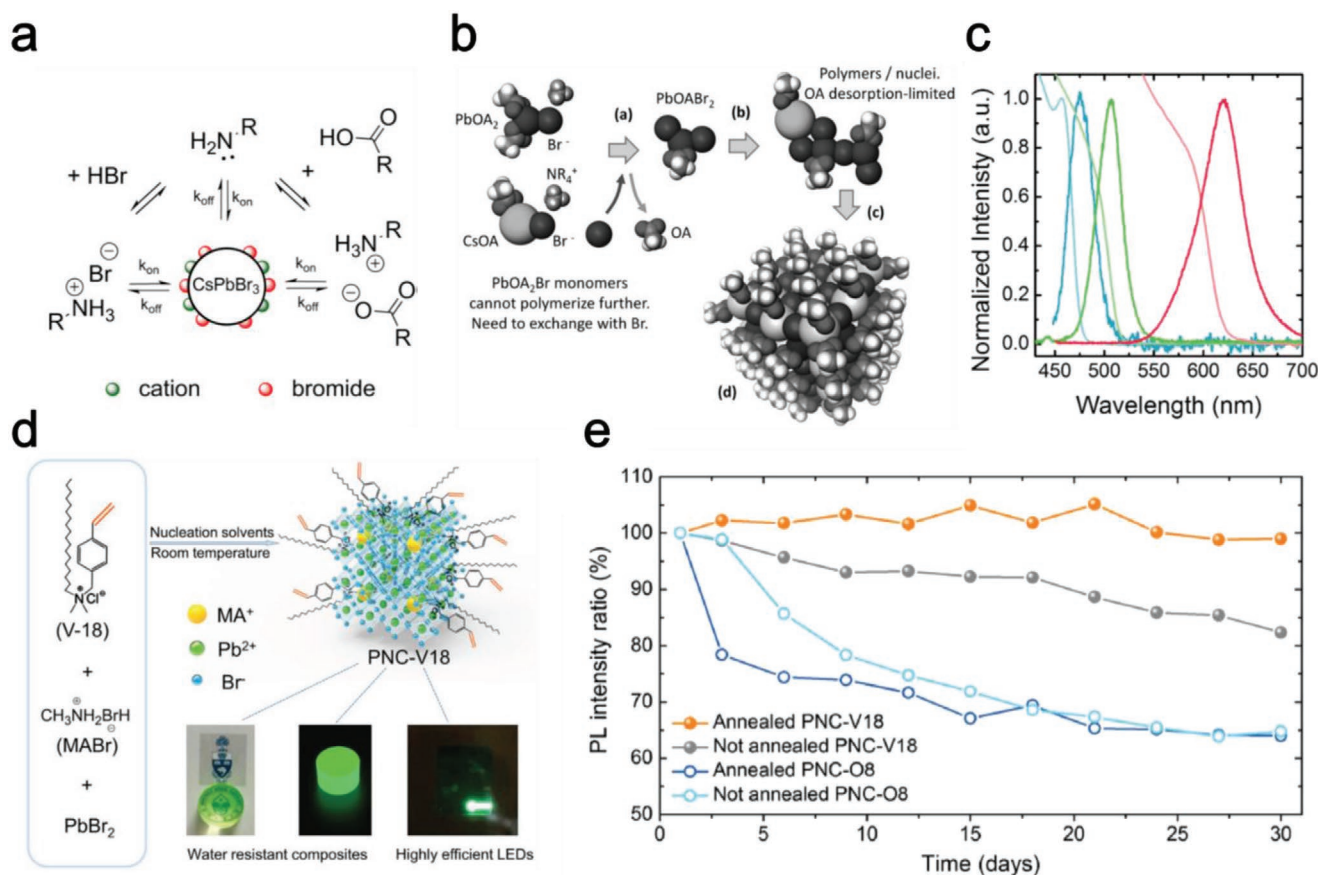


**Figure 8.** a) Schematic illustration of dynamic protonation/deprotonation of ligands on PeNPs surface. Reproduced with permission.<sup>[110]</sup> Copyright 2016 American Chemical Society. b) Synthesis route of the first amine-free PeNPs and c) corresponding absorption and PL spectra of RGB-emitting amine-free PeNPs. Reproduced with permission.<sup>[113]</sup> Copyright 2016, Wiley. d) Method of PeNP synthesis with crosslinkable and polymerizable V18 ligands and their application in water-resistant composites and high-efficiency LEDs. e) PL stability of crosslinked-PeNPs (PNC-V18) and controlled sample (PNC-O8) in ambient condition. Reproduced with permission.<sup>[115]</sup> Copyright 2017, Wiley.

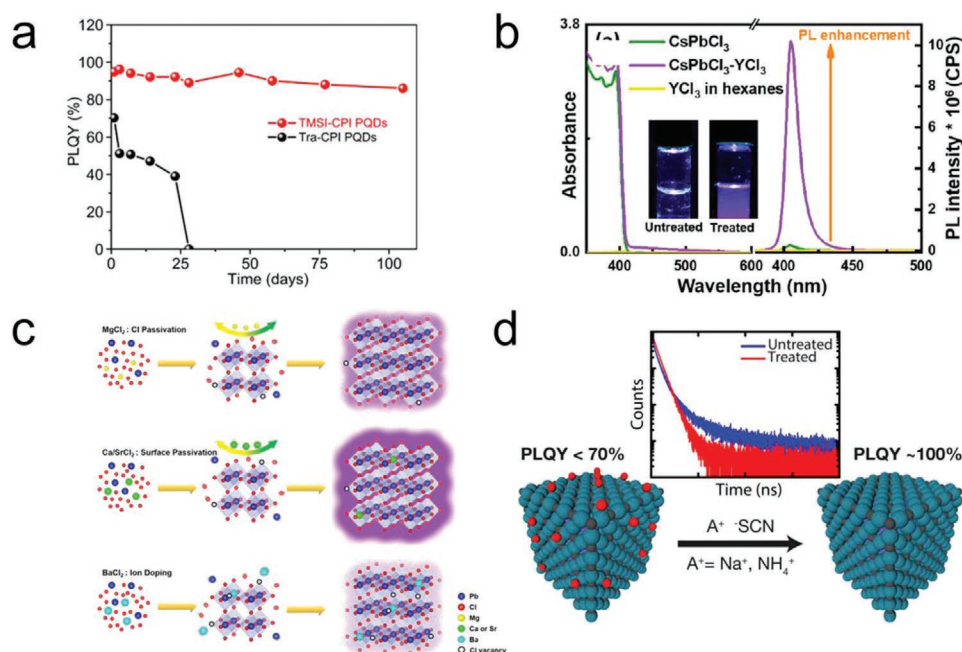


**Figure 9.** a) PLQYs of TMSI-Cspb<sub>3</sub> and traditional CsPb<sub>3</sub> PQDs versus storage time. Reproduced with permission.<sup>[119]</sup> Copyright 2019, American Chemical Society. b) Steady-state optical absorption and PL spectra for CsPbCl<sub>3</sub> NPs before and after YCl<sub>3</sub> surface passivation. Reproduced with permission.<sup>[120]</sup> Copyright 2018, American Chemical Society. c) Schematics of proposed passivation and doping models for various alkaline earth metals. Reproduced with permission.<sup>[122]</sup> Copyright 2019, American Chemical Society. d) Schematic of thiocyanate salt treatment. Reproduced with permission.<sup>[112]</sup> Copyright 2017, American Chemical Society.

OPA-capped PeNP has greatly improved chemical stability during storage under ambient conditions.

Crosslinking of ligands is another ligand-engineering approach to increase the chemical stability of PeNPs. A method to synthesize PeNPs with crosslinkable and polymerizable ligands<sup>[115]</sup> uses 4-vinylbenzyl-dimethyloctadecylammonium chloride ligands with a styryl functional group, which can enable the crosslinking of radical polymerization (Figure 8d).

Crosslinking was accomplished by heating the PeNPs. The crosslinking decreased the surface-defect density and thereby increased the PLQY from 33% to 56%. The PL intensity of crosslinked-PeNPs was unchanged after storage for 30 d in ambient conditions, whereas the uncrosslinked sample maintained only 65% of its initial PL intensity (Figure 8e). Notably, bulk composite fabricated using crosslinked-PeNPs showed extremely high resistance to water without significant change in PL intensity or wavelength after storage for 90 d in water.

### 3.5. Defect Engineering

Although ligand plays a role of passivation of defects on the surface of PeNPs, there are problems that the ligands are easily detached from the NP surfaces<sup>[110]</sup> and resulting defects are difficult to be passivated due to the steric hindrance of the ligand.<sup>[102]</sup> As the particle size decreases, the surface to volume ratio increases, and the surface greatly affects the properties of PeNPs. In particular, the under-coordinated Pb located on the surface acts as a nonradiative trap state,

and this defect deteriorates not only optical properties but also stability of PeNPs.<sup>[116–118]</sup> Therefore, in order to achieve high-efficiency PeNPs, additional passivation strategies are required.

Replacement of the conventional lead with Pb-oleate and of the conventional halide source with trimethylsilyl iodide (TMSI)<sup>[119]</sup> yielded a halide-rich surface of PeNPs with I/Pb molar ratio = 4.2, whereas the standard process that uses PbI<sub>2</sub> as halide source yields I/Pb molar ratio = 2. Under the halide-rich surface, under-coordinated Pb atoms are passivated and CsPbI<sub>3</sub> NPs had PLQY = 85% after storage for 105 d (Figure 9a).

Use of excess halide may also eliminate the lead-rich surface and various metal halides<sup>[119–123]</sup> have been proposed. For example, stable CsPbX<sub>3</sub> (X ∈ {Br, I}) NPs have been synthesized by introducing an additional metal halide (ZnX<sub>2</sub>).<sup>[119]</sup> Compared with pristine CsPbX<sub>3</sub>, ZnX<sub>2</sub>-CsPbX<sub>3</sub> has a surface that is rich in lead halide and were nearly intact after aging for 5 d under ambient atmosphere. Dual-surface passivation of CsPbCl<sub>3</sub> NPs has been achieved using metal halide (YCl<sub>3</sub>).<sup>[120]</sup> Y<sup>3+</sup> and Cl<sup>-</sup> ions efficiently form the surface Pb–Cl ion-pair and passivate under-coordinated Pb, to yield a Cl-rich surface. After YCl<sub>3</sub> treatment, PLQY of CsPbCl<sub>3</sub> NPs increased by a factor of 60 (Figure 9b).

Suitable ion doping<sup>[121–125]</sup> can be used to suppress the formation of surface traps. Various alkaline earth metals (e.g., Ca, Sr, Ba, and Mg) can dope CsPbCl<sub>3</sub> NPs<sup>[122]</sup> (Figure 9c). The location of the dopant and the passivation effect vary depending on the metal species. Ca<sup>2+</sup> and Sr<sup>2+</sup> ions are located on the defect on NP surface and strongly bind with Cl to form a passivation layer that reduces surface traps.

Other methods<sup>[112,126–129]</sup> to passivate defects in PeNPs apply ligands in a postsynthesis process. Treatment with thiocyanate salt yielded CsPbBr<sub>3</sub> NPs that had extremely high PLQY = 100%<sup>[112]</sup> (Figure 9d). Thiocyanate salts partially replaced the surface ligands and formed lead-thiocyanate bonds and thereby decreased the number of under-coordinated lead ions on the surface. The high PLQY of thiocyanate treated CsPbBr<sub>3</sub> was maintained over time, whereas PLQY of untreated samples declined drastically.

## 4. PL Applications

This section demonstrates the possibility of perovskite emitters for commercialization. The process of commercializing perovskite emitters and the adoption of the display structure will likely be similar to those of QDs, so those processes are used as a guideline in the ensuing presentation.

### 4.1. Display Structures for PL Application

QD displays were commercialized by applying a blue-emitting LED on an LCD that uses a BLU; the purpose of this design was to utilize the PL characteristics of existing QDs. Depending on how QDs are applied, they are divided into three structures: “on-chip,” “on-edge,” and “on-surface.” Each structure has advantages and disadvantages and the best method may vary depending on the application area (Figure 10).<sup>[27,129]</sup> Therefore, we will compare the structure and the advantages of the various LCDs and explain the application of perovskite emitters on those devices.

#### 4.1.1. On-Chip Structure

This structure is compatible with the phosphor-converted WLED structure that uses YAG:Ce. This existing optical design structure is the most effective for QD phosphor applications<sup>[130]</sup> and can be used for perovskite emitter without modification; i.e., the LED package can be used as-is by simply replacing the phosphor. However, the LED junction generates a high temperature and the LED emits bright light; both of these phenomena can reduce the lifetime and stability of the PeNP.<sup>[3,27,131]</sup>

#### 4.1.2. On-Edge Structure

In this structure, a resin infused with QDs is injected into the glass tube by exploiting capillarity. A QD glass tube is inserted between the blue-emitting LED bar and the light guide plate (LGP), aligned accurately then fixed in place; a mixing cup made of highly reflective plastic is used to improve efficiency.<sup>[132]</sup> The on-edge structure consisting of LGP, blue LED bars, QD glass tubes, and mixing cups has a trade-off between efficiency and color uniformity.

#### 4.1.3. On-Surface Structure

QD film<sup>[27,133,134]</sup> is most commonly used by attaching it to the light-guide plate. The film can be kept separate from the heat source of the LED, so the operating temperature is similar to room temperature. Also, in this design, the amount of incident light per area is the smallest; the low temperature and low light

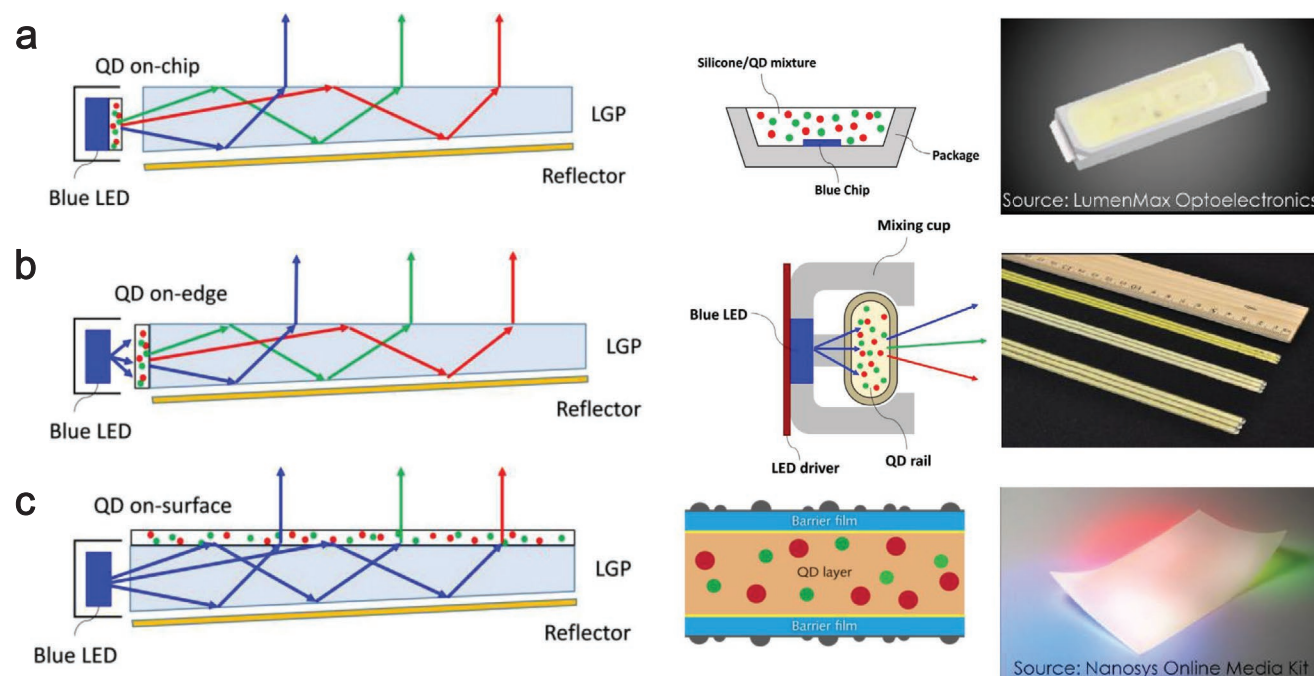


**Figure 10.** Schematics of three display structures implementing QD mixtures. a) QD placed within an LED package. b) QD placed between LED and light guide plate, also known as quantum rail. c) QD (known as quantum dot enhancement film (QDEF)) placed on the top surface of light guide plate (LGP). Left and middle column: Reproduced with permission.<sup>[129]</sup> Copyright 2017, IEEE; Right column: Reproduced with permission.<sup>[27]</sup> Copyright 2015, Wiley.

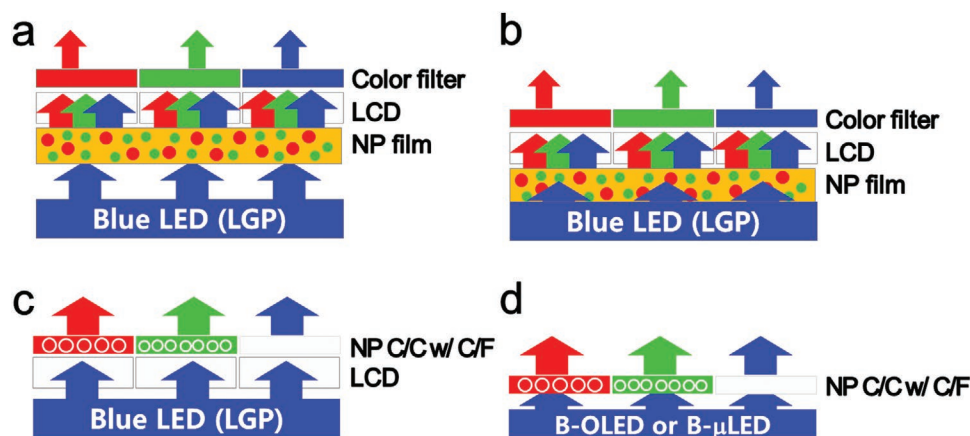


**Figure 11.** Scheme of four types of “on surface” structures. a) Structure currently applied to commercial products and b) NP film laminated directly on glass LGP structure; soon to be commercialized. c) Color conversion (CC) with combined structure color filter (CF) and NP to convert color at CF stage. d) CC structure that uses blue OLED or blue  $\mu$ LED without LGP and blue LED.

intensity greatly improve the reliability and long-term chemical stability of the perovskite emitters.<sup>[47,135]</sup>

QD thin films are also widely used for CFs. This method has been used in CFs that use LCDs, blue-emitting OLEDs, and blue-emitting micro-LEDs (Figure 11). Isotropic release of QDs and PeNPs can greatly widen the viewing angle. Therefore, the CF has the photoemissive effect at the last stage, so the same image quality can be obtained as by using an OLED, but use of QDs in the CF has the disadvantage of increasing the QD consumption by four to ten times compared to the film method.

PeNPs are relatively inexpensive, so use of them can maintain price competitiveness even if a large quantity of them are used. Use of PeNPs is expected to be competitive with use of QDs without any delay caused by trial and error in the commercialization process for display. Commercialized perovskite-emitter-DCD will likely use the on-chip or on-surface applications.

#### 4.2. Perovskite Emitters PL Application Cases

With the on-chip structure wide color gamut can be easily achieved without any special optical design. Some applications have already been developed using red and green PeNPs (Figure 12). One uses a green-emitting MP-CsPbBr<sub>3</sub> PeNPs nanocomposite with red-emitting PeNPs in silicon resin and subjected to excitation by using a blue-emitting InGaN chip to fabricate WLED (Figure 12a). The light from the WLED was passed through a CF. The NTSC value was 113% and the Rec.2020 value was 85%.<sup>[67]</sup> On the Commission internationale de l'éclairage (CIE) chromaticity chart, the color coordinate triangle (Figure 12b)<sup>[71]</sup> drawn by the green-emitting and red-emitting APTES-PeNP/SiO<sub>2</sub>, and blue-emitting chip encompassed 120% of the NTSC-standard, which is better than that achieved using QDs.<sup>[136]</sup> This result demonstrates that the white backlight was excellent. Three resolved PL peaks were observed, in the blue, green, and red spectral regions respectively; this observation demonstrates that the PHPS-derived SiO<sub>2</sub> efficiently prohibited anion exchange between Br<sup>-</sup> and I<sup>-</sup>. By using these RGB components in the electroluminescent (EL)

spectrum, the color gamut of the fabricated WLED was calculated to be 127% of NTSC color space (Figure 11c).<sup>[73]</sup> Moreover, the fabricated WLED showed wide color gamut of 95% of Rec. 2020<sup>[67,137]</sup> (Figure 12c). Red-emitting LEDs and green-emitting LEDs can be manufactured in separate packages, so they can be applied without being subject to anion exchange. Three different cases create encapsulated PeNPs to prevent the spectral change resulting from the anion exchange and increase chemical stability. All cases show better color gamut than NTSC. However, on-chip structure does not provide long-term stability or the reliability because of the high brightness and high operation temperature of the LEDs.

For concept demonstration, a green-emitting PeNP-polymer film and a red-emitting CdSe based QD-polymer film were prepared<sup>[80]</sup> (Figure 13). Overall, the system can cover over 100% of the Adobe RGB color gamut and 95% of the Rec. 2020 color gamut (Figure 13a). A similar approach has recently been commercialized by 3M/Nanosys and QD Vision<sup>[138–142]</sup> with green-emitting and red-emitting QDs.

Hybrid film fabricated using swelling-deswelling micro-encapsulation can overcome the instability of perovskite material. This perovskite film has the advantage of narrow line width (FWHM = 18 nm) of green emission; this narrow band is essentially pure green, which is essential to widen the color gamut.<sup>[80]</sup> Green-emitting PeNPs using core-shell structure for improved stability and Red QDs are dispersed in polymer at the same time. As a proof of concept, Quantum Solutions company fabricated and tested a prototype of PMMA film with Cs<sub>4</sub>PbBr<sub>6</sub> powder and red-emitting CdSe/ZnS QDs<sup>[48,49]</sup> (Figure 13b). This film is semitransparent with yellow illumination under UV. It has a thickness of 200  $\mu$ m and is laminated between two pure PMMA films (100  $\mu$ m thick) to prevent degradation under air and moisture. The PL spectrum of the film consists of two emission peaks with relative intensities of 3:1. The higher one corresponds to Cs<sub>4</sub>PbBr<sub>6</sub> with emission peak at 520  $\pm$  1 nm and narrow FWHM < 20 nm. The smaller one corresponds to CdSe/ZnS QDs with emission peak at 620  $\pm$  1 nm and FWHM > 25 nm. CIE 1931 Chromaticity Diagram for this film (Figure 13b) has a pure green color; the color gamut area is 120% of NTSC area. The big advantage of such film is that the concentration of Pb

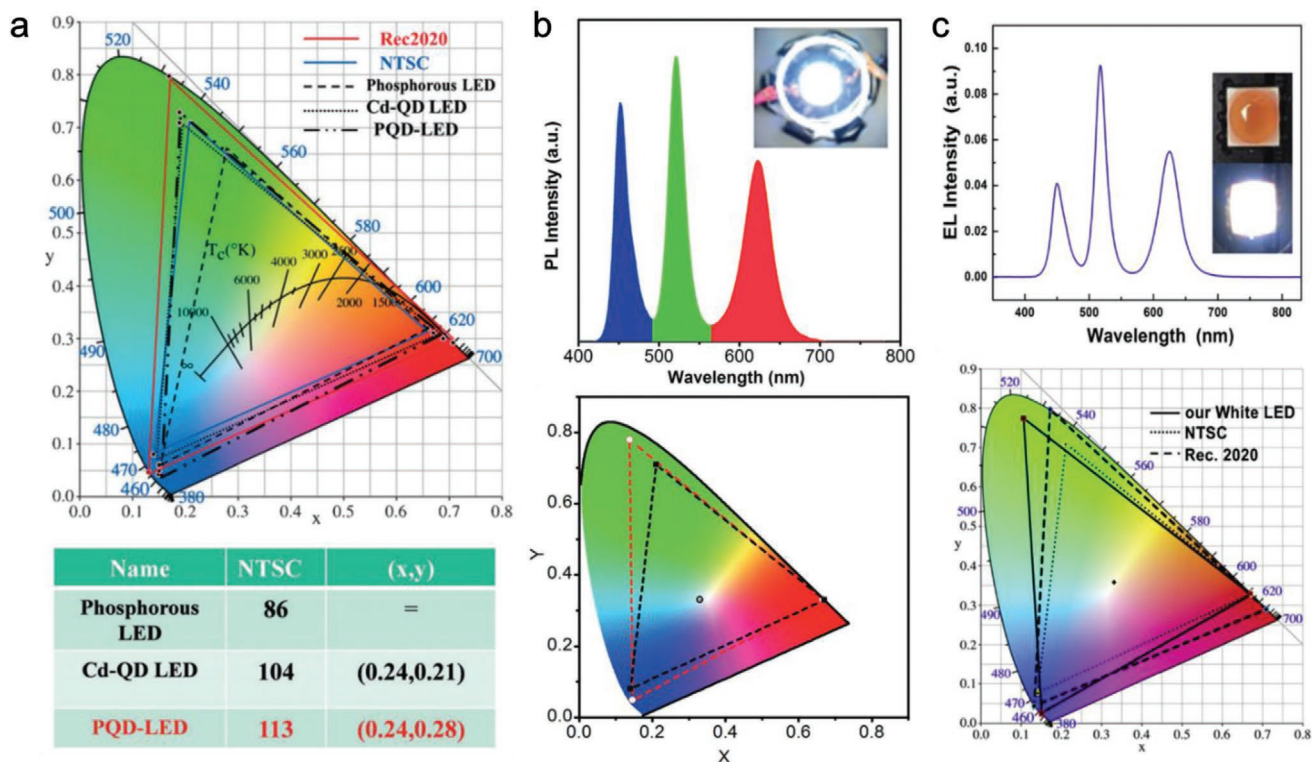


**Figure 12.** a) Down-conversion characteristics of PeNPs encapsulated in mesoporous silica with blue LED. Reproduced with permission.<sup>[67]</sup> Copyright 2016, Wiley. b) PL spectra of the WLED (inset: photograph of device operated at 20 mA) and color triangle of the blue LED, the green and red QD/silica (red dashed line) compared to the NTSC TV standard (black dashed line) and the CIE color coordinates of the WLED. Reproduced with permission.<sup>[71]</sup> Copyright 2016, Wiley. c) PeNP using polysilazane and compared with color reproduction characteristics. Reproduced with permission.<sup>[73]</sup> Copyright 2016, Elsevier.

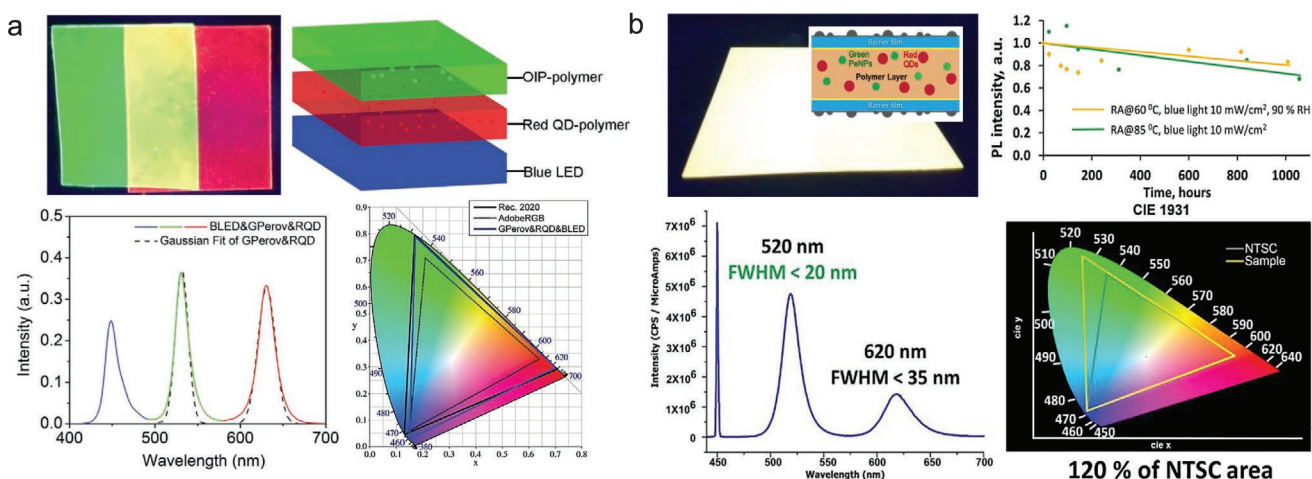


**Figure 13.** a) Application of MAPbBr<sub>3</sub>-polymer composite films as down-converters for back-light units of wide-color-gamut displays. Photograph of red QD-PS and MAPbBr<sub>3</sub>-PS composite films under UV illumination. Scheme of white light generation by integrating red-emitting QD-PS and MAPbBr<sub>3</sub>-PS films with blue-emitting diodes. Emission spectra of a white LED system with green-emitting MAPbBr<sub>3</sub>-PS and red-emitting QD-PS films as down-converters for blue-emitting LEDs. Dashed lines: Gaussian fit for green and red emission spectra. Color gamut coverage of the white LED systems (blue) with adobe RGB (gray) and Rec. 2020 (black) standards for comparison in CIE 1931. Reproduced with permission.<sup>[80]</sup> Copyright 2016, Wiley. b) Green-emitting PeNP to be used as a green emissive material in combination with red-emitting QDs (CdSe or InP QDs based) for LCD backlighting. Due to narrow FWHM of emission, green-emitting PeNPs make LCD to exceed NTSC standards and get it closer to Rec. 2020. Quantum-solutions' special QDs shelling achieves high thermostability and photodegradation resistivity according to industrial standards to QDs. Reproduced with permission.<sup>[48]</sup> Copyright 2019, Wiley.

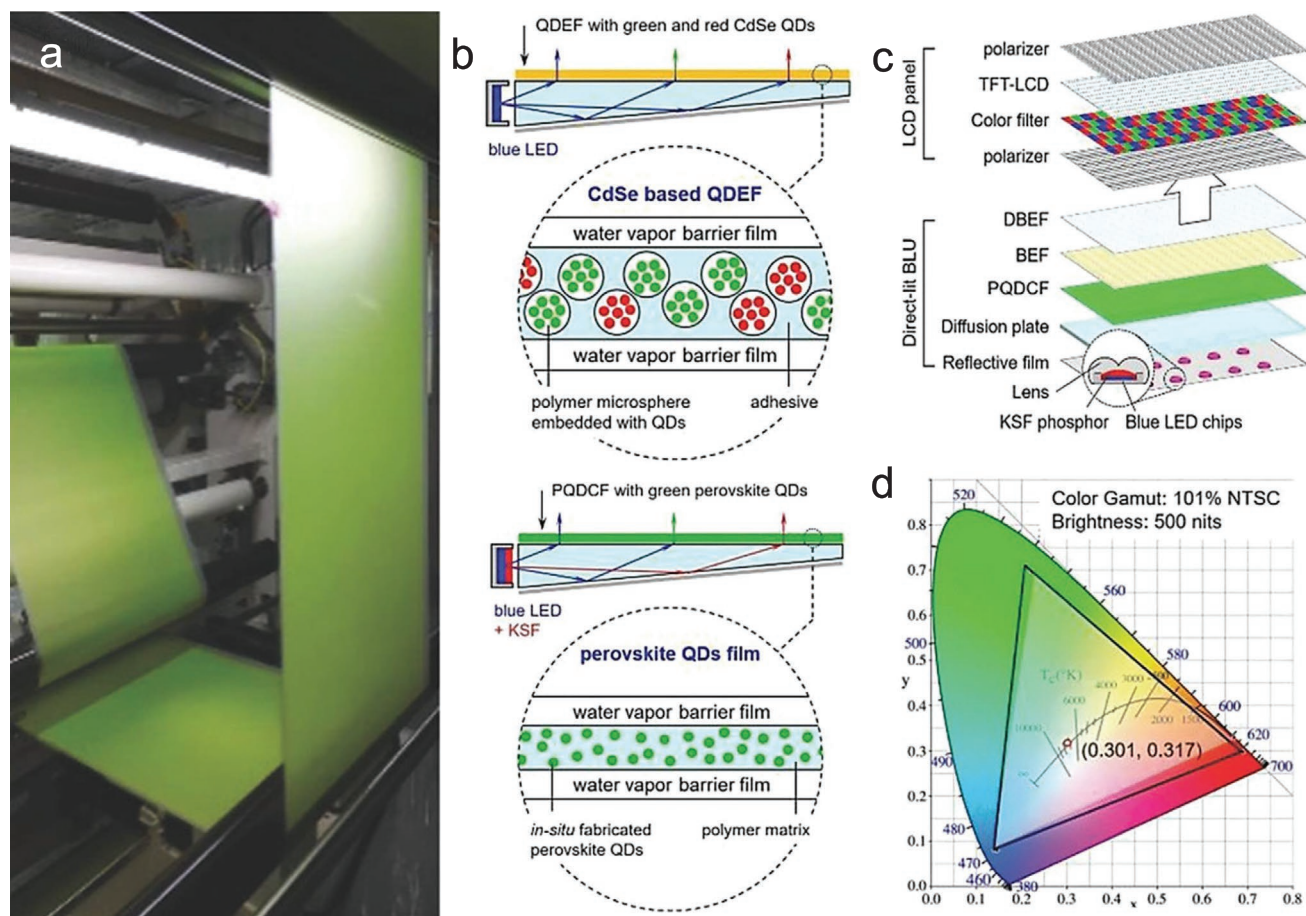


**Figure 14.** a) Large-scale PeNP film fabrication by roll-to-roll technique. b) Comparison of BLU structures and film structures of QDEF and PeNP film. c) The structure diagram of PeNP film-LCD TV prototype. d) The color gamut and white color coordinates of the PeNP film -LCD TV prototype in CIE 1931 diagram. Reproduced with permission.<sup>[139]</sup> Copyright 2018, Wiley.

is <1000 ppm, and the concentration of Cd is < 100 ppm, so it meets the EU RoHS, whereas films that contain only CdSe QDs do not.<sup>[48,49,80,137]</sup>

Quantum-solutions company also performed a harsh-acceleration test by monitoring of PLQY for samples that were treated with continuous illumination under a blue-emitting LED setup with power 10 W for 1000 h. The PLQY and FWHM did not change during this test. This result shows the feasibility of PeNPs for commercialization. However, the proposed LCD had on-surface structure which was adopted to compare with the on-chip structure, and used a hybrid method in which QDs and PeNPs are mixed rather than using PeNPs for both red and green emission. Such cases without hybrid method as in conventional QD LCD cannot prohibit anion exchange between Br<sup>-</sup> and I<sup>-</sup> when two kinds of perovskite particles are dispersed in the same resin. To achieve an affordable display, simplest and cheapest process would be to disperse the same kind of particles for display.<sup>[48,49]</sup>

A practical application that is closest to commercialization (Figure 14) is a prototype TV by TCL Co.<sup>[129–141,143]</sup> Until now, the application examples have prepared PeNP film by using an ex situ method to synthesize NPs and disperse them in resin. The perovskite film was prepared by synthesizing green-emitters by an in situ method using polyvinylidene difluoride (PVDF)

and perovskite precursor in DMF solution to yield a swelling–deswelling process. Perovskite film was applied to blue-emitting LEDs with red-emitting phosphor K<sub>2</sub>SiF<sub>6</sub>:Mn<sup>4+</sup> (KSF) to achieve white light emission and further applied to prototype TVs.

Zhijing Nanotech and Lucky cooperation have developed a roll-to-roll process to scale-up fabrication of PeNP film (Figure 14a); they worked with TCL to demonstrate the first PeNP film integrated for LCD backlights.<sup>[47,135]</sup> In the PeNP film -LCD TV prototype (Figure 14b), the blue light emitted from an LED chip is partly converted to red and green light by a red-emitting KSF phosphor and a green-emitting PeNP film, respectively. Compared with CdSe QDs based QDEF, PeNP film has significant advantages of low costs, high brightness, and low heavy metal content (Figure 13c). In 2018, TCL achieved the first PeNP film based 55" TV panel with a color gamut of 101% and a highest brightness of 500 nits<sup>[139–141,143]</sup> (Figure 14d).

Another approach uses polymer-PeNPs composite films that were obtained using swelling–deswelling microencapsulation that exploits tensile strength. This approach achieved a backlight for an LCD with a color gamut of 89–91% of the Rec. 2020 standard.<sup>[136]</sup> Under adequate tensile force, the PVDF may be stretched and aligned along the force direction; this process leads to spatial alignment of the inclusions within the composite film. The authors exploited this unique mechanical

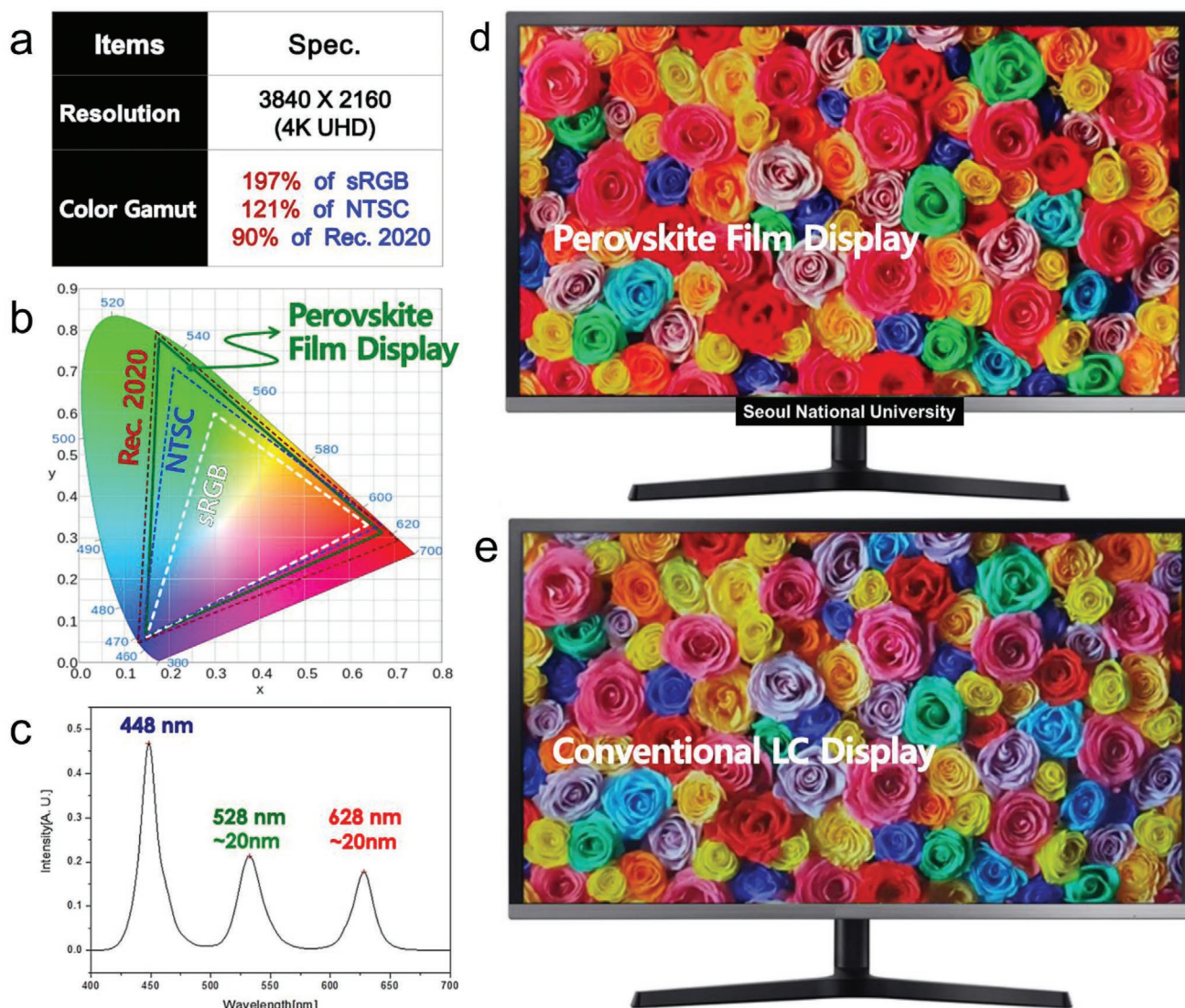


**Figure 15.** A prototype of 28 inch, 4K ultrahigh definition (UHD) LCD/perovskite film display at Consumer Electronics Show (CES) 2020 by Seoul National University. a) Specification of the prototype LCD/perovskite film display. b) Color gamut of perovskite film display in CIE 1931 diagram. c) Spectrum of perovskite film display. d) Prototype of LCD/perovskite film display and e) conventional LCD without the perovskite color conversion film.

property and combined it with in situ fabrication to produce PeNP film.

Recently, the research group at Seoul National University led by Tae-Woo Lee demonstrated an LCD/perovskite film display with 4K (3840 × 2160) resolution at Consumer Electronics Show (CES) 2020 in which a down-conversion film made of green MAPbBr<sub>3</sub> NPs (FWHM ≈ 20 nm) and red CdSe/ZnS core-shell QDs (FWHM ≈ 20 nm) was installed in front of blue LED backlight (**Figure 15**).

## 5. Conclusion and Perspective

We conclude this article by arranging the possible uses of perovskites. Research on PeNPs has sought ways to obtain chemical stability and has made rapid progress. Methods that

improved the stability of PL can be assigned to five types: i) encapsulation in polymer, ii) encapsulation in inorganic material, iii) use of core/shell structure, iv) ligand engineering to control the length and binding energy of the ligand, and v) defect engineering.

Satisfaction of stability and reliability and excellent optical efficiency are essential elements and economic considerations are inevitable for the commercialization. QDs are currently only used for high-end products because of the high cost of material synthesis. When used for CFs in the near future, the consumption of QDs will increase rapidly, so inexpensive emitters are urgently needed. Considering these requirements, we evaluated Cd QDs, InP QDs, and PeNPs by five criteria: i) color gamut, ii) material price, iii) material consumption, and iv) environmental regulation (RoHS regulation), and v) long-term stability (**Figure 16**).

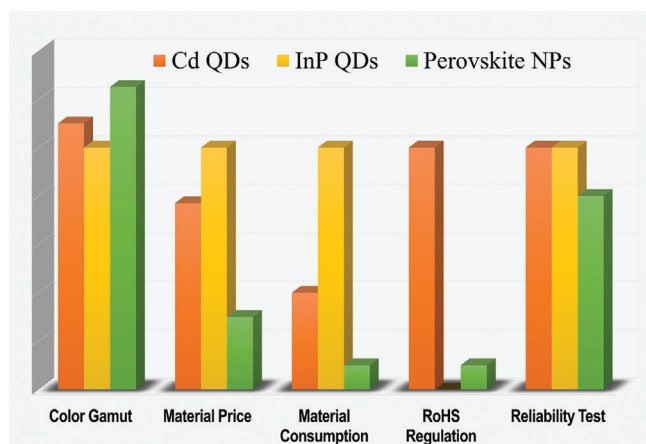


**Figure 16.** Comparison of competitiveness of perovskite emitting materials versus existing quantum dots from an economic viewpoint.

- i) *Color gamut:* The key parameter that determines the color gamut is the emission band width: as band width narrows, the area in color space that can be expressed on the display widens. The PeNPs have much narrower emission band width than those of Cd QDs and InP QDs, so PeNPs are advantageous to widen color reproduction (Table 1: Achievement ratio of Rec. 2020).
- ii) *Material cost:* Perovskites are composed of readily available, inexpensive materials; Cd QDs and InP QDs are more expensive than perovskites.
- iii) *Material consumption:* PeMs mostly in a form of PeNPs have higher absorption coefficient than those of Cd QDs and InP QDs, so fewer PeNPs than Cd QDs or InP QDs are needed to achieve the same brightness. For the same reason, more InP QDs are needed than Cd QDs.
- iv) *Environmental regulation:* RoHS regulations limit Cd content to 100 ppm and Pb content to 1000 ppm, so the Cd QDs are more stringently regulated than the PeMs. The components of InP QDs are not regulated. The regulation of Pb is ten times more relaxed than that of Cd.
- v) *Long-term stability:* PeNPs have about 80% of the reliability of Cd QDs and InP QDs based on how many criteria for commercialization are met. Cd QDs and InP QDs meet all five criteria related to a high luminous flux test (change of less than 15% after 1000 h under stress condition), two types of tests of high temperature and high humidity (60 °C—RH 90 and 85 °C—RH 85), and two different high temperature tests (60 and 85 °C). PeNPs meet four of five criteria (80%) which are two types test of high temperature and high humidity and two types test of two different high temperature conditions but require further improvement at high luminous flux conditions.<sup>[47,49]</sup> Cd QDs are more stable than InP QDs, but both materials are already commercialized and evaluated as equivalent because the difference in stability does not affect consumers.

Optical property of PeNPs is superior or equal to Cd QDs and InP QDs. Therefore, the high luminous flux immunity must be increased to the level required by the industry before perovskite emitters can compete with existing QDs.

Systematic analysis of the trial-and-error process that was involved in producing practical QD light-emitters may identify

ways to speed up the commercialization of display products that use PeNPs. For QDs, a prototype was introduced by a display company 2–3 years after the light-emitting characteristics were discovered. Lessons learned during commercialization of display using QD light-emitters may reduce time delay for PeNPs.

Application of PeNPs films in LCD that use light emitting characteristics has recently been introduced, the film does not use both of red-emitting and green-emitting PeNPs; they combine green-emitting PeNPs with red-emitting Cd QDs, InP QDs, or KSF. Development of 100% PeNP film requires development of a way to prevent diffusion of mobile ions between red-emitting PeNPs and green-emitting PeNPs which yield intermediate emission when they are dispersed together.

A unique characteristic of perovskite emitter is that PeNPs can be synthesized in a polymer with solvents (in situ fabrication); the process steps can be simplified and polymers can be used for encapsulation during the synthesis process without exposing the perovskite to oxygen and moisture in the external environment. However, the color coordinates and brightness must be adjusted according to the purpose of the screen, and the fine-tuning wavelength and the concentration control must be adjusted. Adjustment of precursor concentration for each purpose is not currently feasible. Furthermore, the swelling process may yield non-uniformity of film thickness and of concentration. These issues limit large display application. In addition, PeNP synthesized by the in situ method is difficult to encapsulate individual NP, so different types of NP or two or more different films must be used for display application to the “on-surface structure.” Solving these concerns would be large advances toward useful and productive fabrication.

To prevent emission wavelength shift caused by anion exchange between PeNPs, which can induce consequent broadening of emitting bandwidth, encapsulation must be used to disperse two or more types of PeNP together. The shell of core/shell PeNPs must be optimized to achieve chemical and thermal stability.

For PL applications, ligand engineering can focus on improving the stability of the particles without considering the electrical conductivity as in the EL application side; i.e., ligand engineering should be designed to leave uniform coats of polymer or inorganic substances on the surface of the particles and to maintain high temperature stability when robust encapsulation is achieved using high binding energy of ligand.

Defect engineering can be conducted without sacrificing the original crystal structure and other properties, especially because vacancy control during the synthesis of PeNPs is effective to avoid inducing heteroatoms or other impurities.

A process technology that use powder PeNP should be developed for easy use of both film-type and on-chip methods that can be compatible with CFs, and with direct placement of PeNP in an LED chip. Luminous efficiency and color purity have been improved by securing better optical properties than those of QDs, but the stability has not been improved to the level required by the industry. In this case, we predict that PeNP films will replace QDEF or diffusers, and that the color conversion layer on the CF layer, which consumes a large number of NPs, and enable commercialization at a lower price than those that use conventional QDs.

The use of heavy metals remains a concern. Although ten times more Pb than Cd is allowed by the RoHS regulation, so that PeMs including PeNPs in the color conversion film sheet is much easier to meet RoHS than Cd QDs. However, developing low-lead or lead-free perovskite materials while maintaining excellent optical characteristics<sup>[44,45,143–148]</sup> can be a challenging research direction.

## Acknowledgements

This article is part of the Advanced Materials Technologies Hall of Fame article series, which recognizes the excellent contributions of leading researchers to the field of technology-related materials science. H.L., J.P., and S.K. contributed equally to this work. This work was supported by the National Research Foundation of Korea (NRF) grants funded by the Korea government (Ministry of Science and Information & Communication Technology (ICT)) (NRF-2016R1A3B1908431).

## Conflict of Interest

The authors declare no conflict of interest.

## Keywords

display technology, passivation, photoluminescence application, stability, wide color gamut

Received: February 5, 2020

Revised: April 1, 2020

Published online: August 17, 2020

- [1] H.-T. Huang, Y.-P. Huang, C.-C. Tsai, *J. Disp. Technol.* **2011**, *7*, 44.
- [2] K. Masaoka, Y. Nishida, M. Sugawara, E. Nakasu, *IEEE Trans. Broadcast.* **2010**, *56*, 452.
- [3] S. Coe-Sullivan, W. Liu, P. Allen, J. S. Steckel, *ECS J. Solid State Sci. Technol.* **2013**, *2*, R3026.
- [4] Y. Shirasaki, G. J. Supran, M. G. Bawendi, V. Bulović, *Nat. Photonics* **2013**, *7*, 13.
- [5] K. Bourzac, *Nature* **2013**, *493*, 283.
- [6] Q. Hong, K.-C. Lee, Z. Luo, S.-T. Wu, *Appl. Opt.* **2015**, *54*, 4617.
- [7] J. E. Murphy, F. Garcia-Santamaria, A. A. Setlur, S. Sista, in *SID Symp. Dig. Tech. Pap.*, Wiley, San Jose, CA **2015**, pp. 927–930.
- [8] a) Y.-H. Kim, H. Cho, T.-W. Lee, *Proc. Natl. Acad. Sci. USA* **2016**, *113*, 11695; b) S. Yakunin, L. Protesescu, F. Krieg, M. I. Bodnarchuk, G. Nedelcu, M. Humer, G. De Luca, M. Fiebig, W. Heiss, M. V Kovalenko, *Nat. Commun.* **2015**, *6*, 8056.
- [9] A. S. Verma, A. Kumar, S. R. Bhardwaj, *Phys. Status Solidi B* **2008**, *245*, 1520.
- [10] G. Nedelcu, L. Protesescu, S. Yakunin, M. I. Bodnarchuk, M. J. Grotevent, M. V Kovalenko, *Nano Lett.* **2015**, *15*, 5635.
- [11] F. Reinitzer, *Monatsh. Chem. – Chem. Mon.* **1888**, *9*, 421.
- [12] M. Matsuura, Y. Takafuji, K. Nonomura, F. Funada, T. Wada, *Proc. Soc. Inf. Disp.* **1983**, *5*, 148.
- [13] M. Pope, H. P. Kallmann, P. J. Magnante, *J. Chem. Phys.* **1963**, *38*, 2042.
- [14] W. Helfrich, W. G. Schneider, *Phys. Rev. Lett.* **1965**, *14*, 229.
- [15] A. I. Ekimov, A. L. Efros, A. A. Onushchenko, *Solid State Commun.* **1985**, *56*, 921.
- [16] L. Chen, C.-C. Lin, C.-W. Yeh, R.-S. Liu, *Materials* **2010**, *3*, 2172.
- [17] H. Tamaki, Y. Murazaki, in *Phosphor for White Light-emitting Diodes*, 2nd ed., Phosphor Handbook, Vol. 5, (Eds: W. M. Yen, S. Shionoya, H. Yamamoto), CRC Press, New York **2007**, *5*, pp. 533–543.
- [18] Y. Shimizu, K. Sakano, Y. Noguchi, T. Moriguchi, *US Patent No. 5998925*, **1999**.
- [19] G. Blasse, B. C. Grabmaier, *Luminescent Materials*, Springer-Verlag, London **1994**, pp. 10–32.
- [20] B. Di Bartolo, *Optical Interactions in Solids*, 2nd ed., World Scientific, New Jersey **2010**, pp. 2–17.
- [21] M. J. Anc, N. L. Pickett, N. C. Gresty, J. A. Harris, K. C. Mishra, *ECS J. Solid State Sci. Technol.* **2013**, *2*, R3071.
- [22] X. Yang, D. Zhao, K. S. Leck, S. T. Tan, Y. X. Tang, J. Zhao, H. V. Demir, X. W. Sun, *Adv. Mater.* **2012**, *24*, 4180.
- [23] H. Zhang, N. Hu, Z. Zeng, Q. Lin, F. Zhang, A. Tang, Y. Jia, L. S. Li, H. Shen, F. Teng, Z. Du, *Adv. Opt. Mater.* **2019**, *7*, 1801602.
- [24] N. L. Pickett, N. C. Gresty, M. A. Hines, in *SID Symp. Dig. Tech. Pap.*, Wiley, San Francisco, CA **2016**, pp. 425–427.
- [25] X. Yang, Y. Divayana, D. Zhao, K. Swee Leck, F. Lu, S. Tiam Tan, A. Putu Abiyasa, Y. Zhao, H. Volkan Demir, X. Wei Sun, *Appl. Phys. Lett.* **2012**, *101*, 233110.
- [26] E. Lee, C. Wang, C. Hotz, J. Hartlove, J. Yurek, H. Daniels, Z. Luo, D. Zehnder, in *SID Symp. Dig. Tech. Pap.*, Wiley, San Francisco, CA **2016**, pp. 549–551.
- [27] J. S. Steckel, J. Ho, C. Hamilton, J. Xi, C. Breen, W. Liu, P. Allen, S. Coe-Sullivan, *J. Soc. Inf. Disp.* **2015**, *23*, 294.
- [28] C. Murray, D. J. Norris, M. G. Bawendi, *J. Am. Chem. Soc.* **1993**, *115*, 8706.
- [29] M. A. Hines, P. Guyot-Sionnest, *J. Phys. Chem.* **1996**, *100*, 468.
- [30] B. O. Dabbousi, J. Rodriguez-Viejo, F. V Mikulec, J. R. Heine, H. Mattoussi, R. Ober, K. F. Jensen, M. G. Bawendi, *J. Phys. Chem. B* **1997**, *101*, 9463.
- [31] P. O. Anikeeva, J. E. Halpert, M. G. Bawendi, V. Bulovic, *Nano Lett.* **2009**, *9*, 2532.
- [32] J. Thielen, J. Hillis, J. Van Derlofske, D. Lamb, A. Lathrop, in *SMPTE 2014 Annu. Tech. Conf. Exhib.*, SMPTE, Hollywood, CA, USA **2014**, pp. 1–11.
- [33] R. Zhu, Z. Luo, H. Chen, Y. Dong, S.-T. Wu, *Opt. Express* **2015**, *23*, 23680.
- [34] J. Lim, M. Park, W. K. Bae, D. Lee, S. Lee, C. Lee, K. Char, *ACS Nano* **2013**, *7*, 9019.
- [35] Y. Kim, T. Greco, C. Ippen, A. Wedel, M. S. Oh, C. J. Han, J. Kim, *Nanosci. Nanotechnol. Lett.* **2013**, *5*, 1065.
- [36] S.-H. Lee, K.-H. Lee, J.-H. Jo, B. Park, Y. Kwon, H. S. Jang, H. Yang, *Opt. Mater. Express* **2014**, *4*, 1297.
- [37] S. J. Yang, J. H. Oh, S. Kim, H. Yang, Y. R. Do, *J. Mater. Chem. C* **2015**, *3*, 3582.
- [38] C. Ippen, T. Greco, Y. Kim, C. Pries, J. Kim, M. S. Oh, C. J. Han, A. Wedel, *J. Soc. Inf. Disp.* **2015**, *23*, 285.
- [39] N. L. Pickett, J. A. Harris, N. C. Gresty, in *SID Symp. Dig. Tech. Pap.*, **2015**, Wiley, San Jose, CA pp. 168–169.
- [40] S. Sadasivan, K. Bausemer, S. Corliss, R. Pratt, in *SID Symp. Dig. Tech. Pap.*, Wiley, San Francisco, CA **2016**, pp. 333–335.
- [41] R. E. Brandt, J. R. Poindexter, P. Gorai, R. C. Kurchin, R. L. Z. Hoye, L. Nienhaus, M. W. B. Wilson, J. A. Polizzotti, R. Sereika, R. Žaltauskas, L. C. Lee, J. L. MacManus-Driscoll, M. Bawendi, V. Stevanovic, T. Buonassisi, *Chem. Mater.* **2017**, *29*, 4667.
- [42] Y.-H. Kim, S. Kim, S. H. Jo, T.-W. Lee, *Small Methods* **2018**, *2*, 1800093.
- [43] R. Directive, *Off. J. Eur. Union* **2003**, *13*, L37.
- [44] C. Zhou, H. Lin, Y. Tian, Z. Yuan, R. Clark, B. Chen, L. J. van de Burgt, J. C. Wang, Y. Zhou, K. Hanson, Q. J. Meisner, J. Neu, T. Besara, T. Siegrist, E. Lambers, P. Djurovich, B. Ma, *Chem. Sci.* **2018**, *9*, 586.
- [45] J. Luo, M. Hu, G. Niu, J. Tang, *ACS Appl. Mater. Interfaces* **2019**, *11*, 31575.

- [46] W. Chen, J. Hao, J. Qin, D. Wang, K. Wang, X. Sun, in *SID Symp. Dig. Tech. Pap.*, Wiley, San Francisco, CA **2016**, pp. 556–559.
- [47] J. Thielen, D. Lamb, A. Lemon, J. Tibbits, J. Van Derlofske, E. Nelson, in *SID Symp. Dig. Tech. Pap.*, Wiley, San Francisco, CA **2016**, pp. 336–339.
- [48] J. Pan, L. Sinatra, M. Lutfullin, I. Dursun, O. M. Bakr, in *SID Symp. Dig. Tech. Pap.*, Wiley, Los Angeles, CA **2017**, pp. 83–86.
- [49] L. Sinatra, M. Lutfullin, A. S. Abbas, J. Pan, O. M. Bakr, in *SID Symp. Dig. Tech. Pap.*, Wiley, Los Angeles, CA **2018**, pp. 1681–1684.
- [50] C.-H. Chang, H.-C. Cheng, Y.-J. Lu, K.-C. Tien, H.-W. Lin, C.-L. Lin, C.-J. Yang, C.-C. Wu, *Org. Electron.* **2010**, *11*, 247.
- [51] H.-S. Kim, J.-Y. Seo, N.-G. Park, *ChemSusChem* **2016**, *9*, 2528.
- [52] E. J. Juarez-Perez, Z. Hawash, S. R. Raga, L. K. Ono, Y. Qi, *Energy Environ. Sci.* **2016**, *9*, 3406.
- [53] E. J. Juarez-Perez, L. K. Ono, Y. Qi, *J. Mater. Chem. A* **2019**, *7*, 16912.
- [54] A. Dualeh, N. Tétreault, T. Moehl, P. Gao, M. K. Nazeeruddin, M. Grätzel, *Adv. Funct. Mater.* **2014**, *24*, 3250.
- [55] M. Kulbak, S. Gupta, N. Kedem, I. Levine, T. Bendikov, G. Hodes, D. Cahen, *J. Phys. Chem. Lett.* **2016**, *7*, 167.
- [56] Z. Li, M. Yang, J.-S. Park, S.-H. Wei, J. J. Berry, K. Zhu, *Chem. Mater.* **2016**, *28*, 284.
- [57] M. Kulbak, D. Cahen, G. Hodes, *J. Phys. Chem. Lett.* **2015**, *6*, 2452.
- [58] X. Zhang, H. Liu, W. Wang, J. Zhang, B. Xu, K. L. Karen, Y. Zheng, S. Liu, S. Chen, K. Wang, X. W. Sun, *Adv. Mater.* **2017**, *29*, 1606405.
- [59] E. Mosconi, A. Amat, M. K. Nazeeruddin, M. Grätzel, F. De Angelis, *J. Phys. Chem. C* **2013**, *117*, 13902.
- [60] B. Xu, W. Wang, X. Zhang, W. Cao, D. Wu, S. Liu, H. Dai, S. Chen, K. Wang, X. Sun, *J. Mater. Chem. C* **2017**, *5*, 6123.
- [61] A. Hazarika, Q. Zhao, E. A. Gauding, J. A. Christians, B. Dou, A. R. Marshall, T. Moot, J. J. Berry, J. C. Johnson, J. M. Luther, *ACS Nano* **2018**, *12*, 10327.
- [62] S. Baek, S. Kim, J. Y. Noh, J. H. Heo, S. H. Im, K.-H. Hong, S.-W. Kim, *Adv. Opt. Mater.* **2018**, *6*, 1800295.
- [63] D. Amgar, T. Binyamin, V. Uvarov, L. Etgar, *Nanoscale* **2018**, *10*, 6060.
- [64] H. Cho, Y.-H. Kim, C. Wolf, H.-D. Lee, T.-W. Lee, *Adv. Mater.* **2018**, *30*, 1704587.
- [65] B. Brunetti, C. Cavallo, A. Ciccioli, G. Gigli, A. Latini, *Sci. Rep.* **2016**, *6*, 31896.
- [66] A. Latini, G. Gigli, A. Ciccioli, *Sustainable Energy Fuels* **2017**, *1*, 1351.
- [67] H.-C. Wang, S.-Y. Lin, A.-C. Tang, B. P. Singh, H.-C. Tong, C.-Y. Chen, Y.-C. Lee, T.-L. Tsai, R.-S. Liu, *Angew. Chem., Int. Ed.* **2016**, *55*, 7924.
- [68] D. N. Dirin, L. Protesescu, D. Trummer, I. V. Kochetygov, S. Yakunin, F. Krumeich, N. P. Stadie, M. V. Kovalenko, *Nano Lett.* **2016**, *16*, 5866.
- [69] V. Malgras, S. Tominaka, J. W. Ryan, J. Henzie, T. Takei, K. Ohara, Y. Yamauchi, *J. Am. Chem. Soc.* **2016**, *138*, 13874.
- [70] V. Malgras, J. Henzie, T. Takei, Y. Yamauchi, *Angew. Chem.* **2018**, *130*, 9019.
- [71] C. Sun, Y. Zhang, C. Ruan, C. Yin, X. Wang, Y. Wang, W. W. Yu, *Adv. Mater.* **2016**, *28*, 10088.
- [72] Y. Wang, S. Kalytchuk, Y. Zhang, H. Shi, S. V. Kershaw, A. L. Rogach, *J. Phys. Chem. Lett.* **2014**, *5*, 1412.
- [73] D. H. Park, J. S. Han, W. Kim, H. S. Jang, *Dyes Pigm.* **2018**, *149*, 246.
- [74] H. Hu, L. Wu, Y. Tan, Q. Zhong, M. Chen, Y. Qiu, D. Yang, B. Sun, Q. Zhang, Y. Yin, *J. Am. Chem. Soc.* **2018**, *140*, 406.
- [75] Z. Hu, Z. Liu, Y. Bian, S. Li, X. Tang, J. Du, Z. Zang, M. Zhou, W. Hu, Y. Tian, Y. Leng, *Adv. Opt. Mater.* **2018**, *6*, 1700997.
- [76] S. Guarnera, A. Abate, W. Zhang, J. M. Foster, G. Richardson, A. Petrozza, H. J. Snaith, *J. Phys. Chem. Lett.* **2015**, *6*, 432.
- [77] A. Loiudice, S. Saris, E. Oveisi, D. T. L. Alexander, R. Buonsanti, *Angew. Chem., Int. Ed.* **2017**, *56*, 10696.
- [78] T. Leijtens, B. Lauber, G. E. Eperon, S. D. Stranks, H. J. Snaith, *J. Phys. Chem. Lett.* **2014**, *5*, 1096.
- [79] G. Rainò, A. Landuyt, F. Krieg, C. Bernasconi, S. T. Ochsenbein, D. N. Dirin, M. I. Bodnarchuk, M. V. Kovalenko, *Nano Lett.* **2019**, *19*, 3648.
- [80] Y. Wang, J. He, H. Chen, J. Chen, R. Zhu, P. Ma, A. Towers, Y. Lin, A. J. Gesquiere, S.-T. Wu, Y. Dong, *Adv. Mater.* **2016**, *28*, 10710.
- [81] A. Pan, J. Wang, M. J. Jurow, M. Jia, Y. Liu, Y. Wu, Y. Zhang, L. He, Y. Liu, *Chem. Mater.* **2018**, *30*, 2771.
- [82] S. N. Raja, Y. Bekenstein, M. A. Koc, S. Fischer, D. Zhang, L. Lin, R. O. Ritchie, P. Yang, A. P. Alivisatos, *ACS Appl. Mater. Interfaces* **2016**, *8*, 35523.
- [83] S. Pathak, N. Sakai, F. Wisnivesky Rocca Rivarola, S. D. Stranks, J. Liu, G. E. Eperon, C. Ducati, K. Wojciechowski, J. T. Griffiths, A. A. Haghighirad, A. Pellaroque, R. H. Friend, H. J. Snaith, *Chem. Mater.* **2015**, *27*, 8066.
- [84] K. Ma, X.-Y. Du, Y.-W. Zhang, S. Chen, *J. Mater. Chem. C* **2017**, *5*, 9398.
- [85] W. Cha, H.-J. Kim, S. Lee, J. Kim, *J. Mater. Chem. C* **2017**, *5*, 6667.
- [86] P.-C. Tsai, J.-Y. Chen, E. Ercan, C.-C. Chueh, S.-H. Tung, W.-C. Chen, *Small* **2018**, *14*, 1704379.
- [87] K. Chen, X. Deng, G. Dodekatos, H. Tüysüz, *J. Am. Chem. Soc.* **2017**, *139*, 12267.
- [88] H. Zhang, X. Wang, Q. Liao, Z. Xu, H. Li, L. Zheng, H. Fu, *Adv. Funct. Mater.* **2017**, *27*, 1604382.
- [89] Y. Li, Y. Lv, Z. Guo, L. Dong, J. Zheng, C. Chai, N. Chen, Y. Lu, C. Chen, *ACS Appl. Mater. Interfaces* **2018**, *10*, 15888.
- [90] M. Meyns, M. Perálvarez, A. Heuer-Jungemann, W. Hertog, M. Ibáñez, R. Nafria, A. Genç, J. Arbiol, M. V. Kovalenko, J. Carreras, *ACS Appl. Mater. Interfaces* **2016**, *8*, 19579.
- [91] S. Hou, Y. Guo, Y. Tang, Q. Quan, *ACS Appl. Mater. Interfaces* **2017**, *9*, 18417.
- [92] S. Yang, F. Zhang, J. Tai, Y. Li, Y. Yang, H. Wang, J. Zhang, Z. Xie, B. Xu, H. Zhong, K. Liu, B. Yang, *Nanoscale* **2018**, *10*, 5820.
- [93] Y. H. Song, J. S. Yoo, B. K. Kang, S. H. Choi, E. K. Ji, H. S. Jung, D. H. Yoon, *Nanoscale* **2016**, *8*, 19523.
- [94] W. Xu, Z. Cai, F. Li, J. Dong, Y. Wang, Y. Jiang, X. Chen, *Nano Res.* **2017**, *10*, 2692.
- [95] X. Shen, C. Sun, X. Bai, X. Zhang, Y. Wang, Y. Wang, H. Song, W. W. Yu, *ACS Appl. Mater. Interfaces* **2018**, *10*, 16768.
- [96] R. Xie, U. Kolb, J. Li, T. Basché, A. Mews, *J. Am. Chem. Soc.* **2005**, *127*, 7480.
- [97] S. Bhaumik, S. A. Veldhuis, Y. F. Ng, M. Li, S. K. Muduli, T. C. Sum, B. Damodaran, S. Mhaisalkar, N. Mathews, *Chem. Commun.* **2016**, *52*, 7118.
- [98] S. Wang, C. Bi, J. Yuan, L. Zhang, J. Tian, *ACS Energy Lett.* **2018**, *3*, 245.
- [99] C. Jia, H. Li, X. Meng, H. Li, *Chem. Commun.* **2018**, *54*, 6300.
- [100] J. Park, H. M. Jang, S. Kim, S. H. Jo, T.-W. Lee, *Trends in chem.* **2020**, <https://doi.org/10.1016/j.trechm.2020.07.002>.
- [101] Y.-H. Kim, C. Wolf, Y.-T. Kim, H. Cho, W. Kwon, S. Do, A. Sadhanala, C. G. Park, S.-W. Rhee, S. H. Im, R. H. Friend, T.-W. Lee, *ACS Nano* **2017**, *11*, 6586.
- [102] Y.-H. Kim, G.-H. Lee, Y.-T. Kim, C. Wolf, H. J. Yun, W. Kwon, C. G. Park, T.-W. Lee, *Nano Energy* **2017**, *38*, 51.
- [103] F. Zhang, H. Zhong, C. Chen, X. Wu, X. Hu, H. Huang, J. Han, B. Zou, Y. Dong, *ACS Nano* **2015**, *9*, 4533.
- [104] L. Protesescu, S. Yakunin, M. I. Bodnarchuk, F. Krieg, R. Caputo, C. H. Hendon, R. X. Yang, A. Walsh, M. V. Kovalenko, *Nano Lett.* **2015**, *15*, 3692.
- [105] G. Xing, B. Wu, X. Wu, M. Li, B. Du, Q. Wei, J. Guo, E. K. L. Yeow, T. C. Sum, W. Huang, *Nat. Commun.* **2017**, *8*, 14558.
- [106] S. Kumar, J. Jagielski, N. Kallikounis, Y.-H. Kim, C. Wolf, F. Jenny, T. Tian, C. J. Hofer, Y.-C. Chiu, W. J. Stark, T.-W. Lee, C.-J. Shih, *Nano Lett.* **2017**, *17*, 5277.
- [107] A. S. Berestennikov, Y. Li, I. V. Iorsh, A. A. Zakhidov, A. L. Rogach, S. V. Makarov, *Nanoscale* **2019**, *11*, 6747.

- [108] P. Kumar, C. Muthu, V. C. Nair, K. S. Narayan, *J. Phys. Chem. C* **2016**, *120*, 18333.
- [109] Y.-H. Kim, C. Wolf, H. Kim, T.-W. Lee, *Nano Energy* **2018**, *52*, 329.
- [110] J. De Roo, M. Ibáñez, P. Geiregat, G. Nedelcu, W. Walravens, J. Maes, J. C. Martins, I. Van Driessche, M. V Kovalenko, Z. Hens, *ACS Nano* **2016**, *10*, 2071.
- [111] J. Pan, L. N. Quan, Y. Zhao, W. Peng, B. Murali, S. P. Sarmah, M. Yuan, L. Sinatra, N. M. Alyami, J. Liu, E. Yassitepe, Z. Yang, O. Voznyy, R. Comin, M. N. Hedhili, O. F. Mohammed, Z. H. Lu, D. H. Kim, E. H. Sargent, O. M. Bakr, *Adv. Mater.* **2016**, *28*, 8718.
- [112] B. A. Koscher, J. K. Swabeck, N. D. Bronstein, A. P. Alivisatos, *J. Am. Chem. Soc.* **2017**, *139*, 6566.
- [113] E. Yassitepe, Z. Yang, O. Voznyy, Y. Kim, G. Walters, J. A. Castañeda, P. Kanjanaboos, M. Yuan, X. Gong, F. Fan, J. Pan, S. Hoogland, R. Comin, O. M. Bakr, L. A. Padilha, A. F. Nogueira, E. H. Sargent, *Adv. Funct. Mater.* **2016**, *26*, 8757.
- [114] Y. Tan, Y. Zou, L. Wu, Q. Huang, D. Yang, M. Chen, M. Ban, C. Wu, T. Wu, S. Bai, T. Song, Q. Zhang, B. Sun, *ACS Appl. Mater. Interfaces* **2018**, *10*, 3784.
- [115] H. Sun, Z. Yang, M. Wei, W. Sun, X. Li, S. Ye, Y. Zhao, H. Tan, E. L. Kynaston, T. B. Schon, H. Yan, Z.-H. Lu, G. A. Ozin, E. H. Sargent, D. S. Seferos, *Adv. Mater.* **2017**, *29*, 1701153.
- [116] S. Seth, T. Ahmed, A. De, A. Samanta, *ACS Energy Lett.* **2019**, *4*, 1610.
- [117] M. C. Brennan, S. Draguta, P. V Kamat, M. Kuno, *ACS Energy Lett.* **2018**, *3*, 204.
- [118] M. Lai, A. Obliger, D. Lu, C. S. Kley, C. G. Bischak, Q. Kong, T. Lei, L. Dou, N. S. Ginsberg, D. T. Limmer, P. Yang, *Proc. Natl. Acad. Sci. USA* **2018**, *115*, 11929.
- [119] a) J. Y. Woo, Y. Kim, J. Bae, T. G. Kim, J. W. Kim, D. C. Lee, S. Jeong, *Chem. Mater.* **2017**, *29*, 7088; b) Y. Cai, H. Wang, Y. Li, L. Wang, Y. Lv, X. Yang, R.-J. Xie, *Chem. Mater.* **2019**, *31*, 881.
- [120] G. H. Ahmed, J. K. El-Demellawi, J. Yin, J. Pan, D. B. Velusamy, M. N. Hedhili, E. Alarousu, O. M. Bakr, H. N. Alshareef, O. F. Mohammed, *ACS Energy Lett.* **2018**, *3*, 2301.
- [121] M. Lu, X. Zhang, Y. Zhang, J. Guo, X. Shen, W. W. Yu, A. L. Rogach, *Adv. Mater.* **2018**, *30*, 1804691.
- [122] J.-K. Chen, J.-P. Ma, S.-Q. Guo, Y.-M. Chen, Q. Zhao, B.-B. Zhang, Z.-Y. Li, Y. Zhou, J. Hou, Y. Kuroiwa, C. Moriyoshi, O. M. Bakr, J. Zhang, H.-T. Sun, *Chem. Mater.* **2019**, *31*, 3974.
- [123] N. Mondal, A. De, A. Samanta, *ACS Energy Lett.* **2019**, *4*, 32.
- [124] M. Lu, X. Zhang, X. Bai, H. Wu, X. Shen, Y. Zhang, W. Zhang, W. Zheng, H. Song, W. W. Yu, A. L. Rogach, *ACS Energy Lett.* **2018**, *3*, 1571.
- [125] Y. Liu, G. Pan, R. Wang, H. Shao, H. Wang, W. Xu, H. Cui, H. Song, *Nanoscale* **2018**, *10*, 14067.
- [126] B. J. Bohn, Y. Tong, M. Gramlich, M. L. Lai, M. Döblinger, K. Wang, R. L. Z. Hoyer, P. Müller-Buschbaum, S. D. Stranks, A. S. Urban, L. Polavarapu, J. Feldmann, *Nano Lett.* **2018**, *18*, 5231.
- [127] T. Ahmed, S. Seth, A. Samanta, *Chem. Mater.* **2018**, *30*, 3633.
- [128] F. Li, Y. Liu, H. Wang, Q. Zhan, Q. Liu, Z. Xia, *Chem. Mater.* **2018**, *30*, 8546.
- [129] H. Chen, J. He, S.-T. Wu, *IEEE J. Sel. Top. Quantum Electron.* **2017**, *23*, 1900611.
- [130] J. Jang, D.-E. Yoon, S.-M. Kang, Y. H. Kim, I. Lee, H. Lee, Y. H. Kim, D. C. Lee, B.-S. Bae, *Nanoscale* **2019**, *11*, 14887.
- [131] Y. Zhao, C. Riemersma, F. Pietra, R. Koole, C. de Mello Donegá, A. Meijerink, *ACS Nano* **2012**, *6*, 9058.
- [132] K. Twietmeyer, S. Sadasivan, *J. Soc. Inf. Disp.* **2016**, *24*, 312.
- [133] J. Chen, V. Hardev, J. Hartlove, J. Hofler, E. Lee, *SID Symp. Dig. Tech. Pap.*, Wiley, San Francisco Vol. 43, **2012**, p. 895.
- [134] H. Y. Kim, D.-E. Yoon, J. Jang, D. Lee, G.-M. Choi, J. H. Chang, J. Y. Lee, D. C. Lee, B.-S. Bae, *J. Am. Chem. Soc.* **2016**, *138*, 16478.
- [135] a) M. Lutfullin, L. Sinatra, O. Bakr, presented at 10th Int. Conf. Mater. Adv. Technol. (ICMAT), Singapore, June **2019**; b) L. Sinatra, M. Lutfullin, S. L. Mozo, J. Pan, O. Bakr, *SID Symp. Dig. Tech. Pap.*, Vol. 50, Wiley, San Jose **2019**, p. 1712.
- [136] E. Jang, S. Jun, H. Jang, J. Lim, B. Kim, Y. Kim, *Adv. Mater.* **2010**, *22*, 3076.
- [137] Radio Regulations Articles, International Telecommunication Union, Geneva **2012**, <http://search.itu.int/history/HistoryDigitalCollectionDocLibrary/1.41.48.en.101.pdf>.
- [138] J. Chen, V. Hardev, J. Yurek, *Inf. Disp.* **2013**, *29*, 12.
- [139] S. Chang, Z. Bai, H. Zhong, *Adv. Opt. Mater.* **2018**, *6*, 1800380.
- [140] N. Chen, Z. Bai, Z. Wang, H. Ji, R. Liu, C. Cao, H. Wang, F. Jiang, H. Zhong, *SID Symp. Dig. Tech. Pap.*, Vol. 49, Wiley, Los Angeles **2018**, p. 1657.
- [141] H. Ji, H. Xu, F. Jiang, Z. Bai, H. Zhong, *SID Symp. Dig. Tech. Pap.*, Vol. 50, Wiley, San Jose **2019**, p. 411.
- [142] J. Chen, S. Gensler, J. Hartlove, J. Yurek, E. Lee, J. Thielen, J. Van Derlofske, J. Hillis, G. Benoit, J. Tibbits, *SID Symp. Dig. Tech. Pap.*, Vol. 46, Wiley, San Jose **2015**, p. 173.
- [143] J. V. Derlofske, G. Benoit, A. Lathrop, D. Lamb, in *Proc. 20th Int. Disp. Work*, Society for Information Display, Sapporo, Japan **2013**, p. 548.
- [144] J. He, H. Chen, H. Chen, Y. Wang, S.-T. Wu, Y. Dong, *Opt. Express* **2017**, *25*, 12915.
- [145] F. Hao, C. C. Stoumpos, D. H. Cao, R. P. H. Chang, M. G. Kanatzidis, *Nat. Photonics* **2014**, *8*, 489.
- [146] F. Giustino, H. J. Snaith, *ACS Energy Lett.* **2016**, *1*, 1233.
- [147] T. C. Jellicoe, J. M. Richter, H. F. J. Glass, M. Tabachnyk, R. Brady, S. E. Dutton, A. Rao, R. H. Friend, D. Credginton, N. C. Greenham, M. L. Böhm, *J. Am. Chem. Soc.* **2016**, *138*, 2941.
- [148] J. Luo, X. Wang, S. Li, J. Liu, Y. Guo, G. Niu, L. Yao, Y. Fu, L. Gao, Q. Dong, C. Zhao, M. Leng, F. Ma, W. Liang, L. Wang, S. Jin, J. Han, L. Zhang, J. Etheridge, J. Wang, Y. Yan, E. H. Sargent, *Nature* **2018**, *563*, 541.